ODYSSEAS N. KOPSIDAS

Economist – Civil Engineer MSc, PhD Candidate

SCALE UP OF ADSORPTION IN FIXED-BED COLUMN SYSTEMS

Piraeus 2016

Οδυσσέας Κοψιδάς

Copyright 2015

ISBN :

Απαγορεύεται η ανατύπωση ολική ή μερική χωρίς την έγγραφη άδεια του συγγραφέα

SCALE UP OF ADSORPTION IN FIXED-BED COLUMN SYSTEMS

Summary

This work is concerned with the presentation of the scaling up the adsorption process in fixed-bed (or packed-bed) column systems .

These systems are applied, mainly aiming to the removal of heavy metals and other toxics from industrial and municipal effluents.

In Chapter 1, the definitions for fixed-bed adsorption columns systems and the theory for the design of these systems is presented.

In Chapter 2, the modeling of the adsorption process in fixed-bed column adsorption systems is analysed.

The scale up, the mass transfer process, the breakthrough curve, and, especially, the modeling of the breakthrough curve is presented thoroughly.

In the whole work, an emphasis is given in **biosorption processes,** which are a modern aspect of today's Chemical Engineering Technology projects.

Also, in the same chapter, a completed example of the modeling of the breakthrough curve in a specific system is given.

In chapter 3, the role of modeling the fixed-bed column adsorption process in the scale up of such systems is presented in detail.

Presented are the main models, applied today in various projects, in order to gain understanding for the fundamental role of the modeling the breakthrough curve in every system, to have a proper scale up.

In Chapter 4, the biomass as absorbent and the biosorption technology is emphasized.

Also, two case studies are presented in detail.

Finally, the Conclusions from this work are given and the pertinent Bibliography.

CHAPTER 1: INTRODUCTION TO THE FIXED-BED COLUMN SYSTEMS

1.1.Introduction

In chemical processing, a **fixed-bed** or **packed-bed** is a hollow tube, pipe, or other vessel that is filled with a packing material. The packing can be randomly filled with small objects like Raschig rings or else it can be a specifically designed structured packing. Fixed beds may also contain catalyst particles or adsorbents such as zeolite pellets, granular activated carbon, etc.[1].

The purpose of a fixed bed is typically to improve contact between two phases in a chemical or similar process. Fixed beds can be used in a chemical reactor, a distillation process, or a scrubber, but packed beds have also been used to store heat in chemical plants. In this case, hot gases are allowed to escape through a vessel that is packed with a refractory material until the packing is hot. Air or other cool gas is then fed back to the plant through the hot bed, thereby pre-heating the air or gas feed.

The column can be filled with random dumped packing (creating a '"random packed column"') or with (structured packing) sections, which are arranged or stacked (creating a '"stacked packed column"') [1].

In the column, liquids tend to wet the surface of the packing and the vapors pass across this wetted surface, where (mass transfer) takes place. Packing material can be used instead of trays to improve separation in distillation columns. Packing offers the advantage of a lower pressure drop across the column (when compared to plates or trays), which is beneficial while operating under vacuum.

Differently shaped packing materials have different surface areas and void space between the packing. Both of these factors affect packing performance.

Another factor in performance, in addition to the packing shape and surface area, is the liquid and vapor distribution that enters the packed bed. The number of theoretical plates (theoretical stages) required to make a given separation is calculated using a specific vapor to liquid ratio.[1].

If the liquid and vapor are not evenly distributed across the superficial tower area as it enters the packed bed, the liquid to vapor ratio will not be correct and the required separation will not be achieved. The packing will appear to not be working properly. The "height equivalent to a theoretical plate" (HETP) will be greater than expected. The problem is not the packing itself but the mal-distribution of the fluids entering the packed bed.

These columns can contain liquid distributors and redistributors which help to distribute the liquid evenly over a section of packing, increasing the efficiency of the mass transfer. The design of the liquid distributors used to introduce the feed and reflux to a packed bed is critical to making the packing perform at maximum efficiency.

Packed columns have a continuous vapor-equilibrium curve, unlike conventional tray distillation in which every tray represents a separate point of vapor-liquid equilibrium. However, when modeling packed columns it is useful to compute a number of theoretical plates to denote the separation efficiency of the packed column with respect to more traditional trays.

In design, the number of necessary theoretical equilibrium stages is first determined and then the packing height equivalent to a theoretical plate (theoretical equilibrium stage), known as the "height equivalent to a theoretical plate" (HETP), is also determined. The total packing height required is the number theoretical stages multiplied by the HETP[1].

1.2.Column structure: random and stacked packed columns

The column can be filled with random dumped packing (creating a '"random packed column"') or with structured packing sections, which are arranged or stacked (creating a "stacked packed column"'). In the column, liquids tend to wet the surface of the packing and the vapors pass across this wetted surface, where mass transfer takes place [1,2].

Packing material can be used instead of trays to improve separation in distillation columns. Packing offers the advantage of a lower pressure drop across the column (when compared to plates or trays), which is beneficial while operating under vacuum. Differently shaped packing materials have different surface areas and void space between the packing. Both of these factors affect packing performance[2].

1.3.Liquid and vapor distribution (vapor to liquid ratio)

Another factor in performance, in addition to the packing shape and surface area, is the liquid and vapor distribution that enters the packed bed. The number of theoretical stages required to make a given separation is calculated using a specific vapor to liquid ratio. If the liquid and vapor are not evenly distributed across the superficial tower area as it enters the packed bed, the liquid to vapor ratio will not be correct and the required separation will not be achieved.

The packing will appear to not be working properly. The height equivalent to a theoretical plate (HETP) will be greater than expected. The problem is not the packing itself but the mal-distribution of the fluids entering the packed bed. These columns can contain liquid distributors and redistributors which help to distribute the liquid evenly over a section of packing, increasing the efficiency of the mass transfer.[1] The design of the liquid distributors used to introduce the feed and reflux to a packed bed is critical to making the packing perform at maximum efficiency[2].

1.4.Packed column vapor-equilibrium curve

Packed columns have a continuous vapor-equilibrium curve, unlike conventional tray distillation in which every tray represents a separate point of vapor-liquid equilibrium. However, when modeling packed columns it is useful to compute a number of theoretical plates to denote the separation efficiency of the packed column with respect to more traditional trays [1,2].

In design, the number of necessary theoretical equilibrium stages is first determined and then the packing height equivalent to a theoretical equilibrium stage, known as the height equivalent to a theoretical plate (HETP), is also determined. The total packing height required is the number theoretical stages multiplied by the HETP [2].

1.5.Packed bed reactors

Packed bed reactors can be used in chemical reaction. These reactors are tubular and are filled with solid catalyst particles, most often used to catalyze gas reactions.[2] The chemical reaction takes place on the surface of the catalyst [1].

The advantage of using a packed bed reactor is the higher conversion per weight of catalyst than other catalytic reactors. The reaction rate is based on the amount of the solid catalyst rather than the volume of the reactor.

1.6.Theory

The **Ergun equation**, derived by the Turkish chemical engineer Sabri Ergun in 1952, expresses the friction factor in a packed column as a function of the Reynolds number [4] :

$$f_p = \frac{150}{Gr_p} + 1.75 \qquad \text{(eq.1.1)}$$

where f_p and Gr_p are defined as :

$$f_p = \frac{\Delta p}{L}\frac{D_p}{\rho V_s^2}\left(\frac{\epsilon^3}{1-\epsilon}\right) \quad \text{and} \quad Gr_p = \frac{D_p V_s \rho}{(1-\epsilon)\mu} \qquad \text{(eq.1.2)}$$

where:

Δp = the pressure drop across the bed

L = the length of the bed (not the column)

D_p = the equivalent spherical diameter of the packing

ρ = the density of fluid

μ = the dynamic viscosity of the fluid

V_s = the superficial velocity (i.e. the velocity that the fluid would have through the empty tube at the same volumetric flow rate)

ϵ = the void fraction of the bed (bed porosity at any time)

The **Kozeny–Carman equation** is a relation used in the field of fluid dynamics to calculate the pressure drop of a fluid flowing through a packed bed of solids. It is

named after Josef Kozeny and Philip C. Carman. The equation is only valid for laminar flow [5,6].

The equation is given as:

$$\frac{\Delta p}{L} = \frac{180 \bar{V}_0 \mu}{\Phi_s^2 D_p^2} \frac{(1-\epsilon)^2}{\epsilon^3}$$

(eq.1.3)

Where :

Δp = the pressure drop

L = the total height of the bed

$\bar{V}_0$ = the superficial or "empty-tower" velocity

μ = the dynamic viscosity of the fluid

ϵ = the porosity of the bed

Φ_s = the sphericity of the particles in the packed bed

D_p = the diameter of the related spherical particle

This equation holds for flow through packed beds with particle Reynolds numbers up to approximately 1.0, after which point frequent shifting of flow channels in the bed causes considerable kinetic energy losses.

This equation can be expressed as "*flow is proportional to the pressure drop and inversely proportional to the fluid viscosity*", which is known as Darcy's law.[1]

1.7. Packed Column Design

Packed columns are most frequently used to remove contaminants from a gas stream (adsorption). However, packed columns can also be used to remove volatile components from a liquid stream by contacting it with an inert gas (stripping). They are also used in distillation applications where the separation is particularly difficult due to close boiling components. **(http://www.cheresources.com/content/articles/separation-tech)**

The equilibrium data between the contaminant and the solvent (or the distillation components) is needed for the analysis.

If tabulated data for your system is unavailable and the total amount of the contaminant is small (as it usually will be), Raoult's Law can be used to estimate the equilibrium data for absorption or stripping applications. For distillation, equilibrium data can be predicted by selecting the appropriate thermodynamic model. The operating line for the tower is constructed differently depending on whether you're dealing with distillation or adsorption/stripping [1,3].

Since we're focusing on adsorption, we'll use it as an example. In adsorption/stripping, the operating line is constructed differently depending on whether the contaminated stream can be considered "dilute" or if it must be treated as a concentrated stream. Usually, it is safe to treat the stream as dilute if the contaminant makes up less than 10 mole percent of the stream. For streams that cannot be considered dilute, the mass transfer coefficients must be evaluated in terms of the gas and liquid flows. Then, graphical evaluation of several integral relationships must be completed. The description of this process is beyond the scope of this text.

In the figure 1.1 below the general arrangement of a fixed-bed column is presented

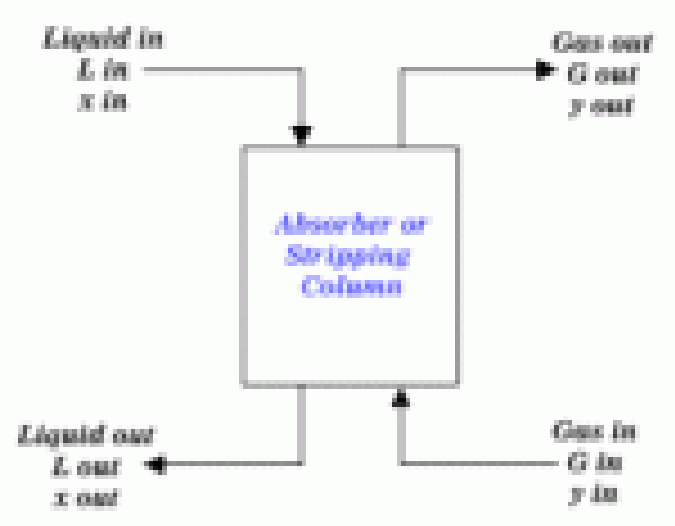

Figure 1.1. General Packed Column Arrangement **(http://www.cheresources.com/content/articles/separation-tech)**

Dilute streams allow the column designer to assume constant mass transfer and the operating line can be constructed in terms of the simplified balance shown below:

$$L_{out}\, x_{out} + G_{out}\, y_{out} = L_{in}\, x_{in} + G_{in}\, y_{in}$$

(eq.1.4)

Where :

L= the feed of the liquid scrubber
G= the feed of the gas, which contains the substance(s) to be removed
x= mole fraction of a component in the liquid phase
y= mole fraction of a component in the gas (vapor) phase

Example 1.1

Suppose you wish to remove acetone from a gas stream of 10,000 mol/h in a fixed - bed column. The inlet gas contains 2.6 mole percent acetone and the outlet gas stream can contain no more than 0.5 mole percent acetone. Assume a pure water stream enters the packed tower at a rate of 8,000 mol/h [2].
The arrangement of this process is presented below:

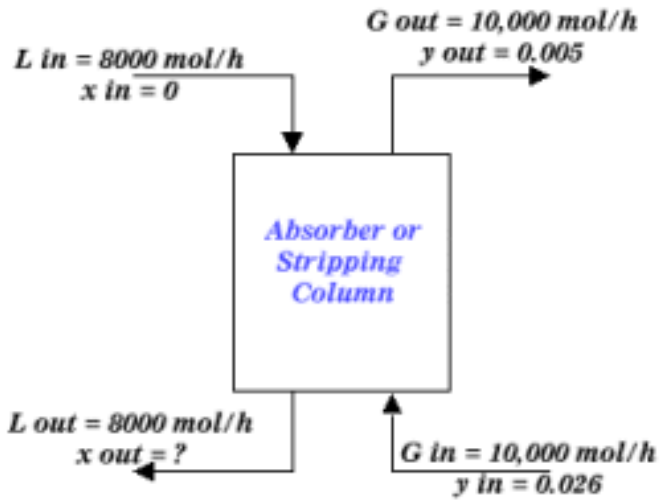

Figure 1.2. Fixed-bed column for the example 1.1. [2].

From the equation 1.4 above, we have:

$L_{out} x_{out} + G_{out} y_{out} = L_{in} x_{in} + G_{in} y_{in}$

$(8000) x_{out} + (10000)(0.005) = (8000)(0)+(10000)(0.026)$

$x_{out} = 0.02625$

The equilibrium and operating lines are constructed as follows:

The equilibrium stages are stepped off between the two lines. Note that for stripping, the operating line would be on the other side of the equilibrium line.

Once the theoretical number of stages have been determined, you can proceed with the design of the column by following the three steps that we'll outline below [2].

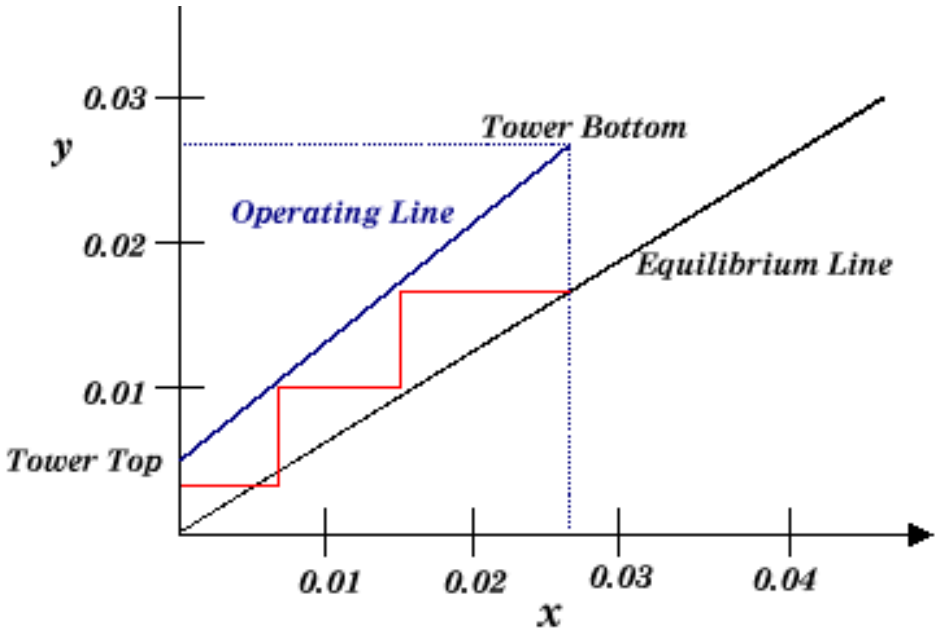

Figure1.3.Constructing the Operating and Equilibrium Lines [2].

CHAPTER 2: MODELING THE ADSORPTION PROCESS IN FIXED-BED COLUMN SYSTEMS

2.1. Introduction

It is well known today, that in every adsorption process, the material from the fixed-bed column is made off, is called adsorbent, whereas the substance being adsorbed is called adsorbate. [7].

The factors influencing strongly the adsorption ability of different adsorbents are the following:

- available surface area,
- polarity,
- contact time,
- pH
- the degree of hydrophilic nature of the adsorbent and adsorbate (Suzuki, 1990).

Thus, the first step in a research or industry project dealing with such systems, is the selection of the proper adsorbent in every case.

In this framework, studies should be firstly focused on batch systems in equilibrium and isotherms should be constructed [8].

In these systems, equilibrium condition is attained when the concentration of the solute remains constant, as a result of zero net transfer of solute adsorbed and desorbed from the adsorbent surface.

The equilibrium adsorption isotherms describe these relationships between the equilibrium concentration of the adsorbate in the solid and liquid phase at constant temperature. Experimental data may provide different isotherm shapes such as: Linear, Favorable, Strongly favorable, Irreversible and Unfavorable as shown in Figure 2.1.[9].

Of course, the linear isotherm starts from the origin in the q_{eq} vs.C_{eq} adsorption plot.

Usually, the adsorbent related to this isotherm is chosen because the linear isotherm facilitates the column modeling although it does not show a specific selectivity 10].

Adsorbents that give isotherms with strong upward curvature are called as favorable and strongly favorable. These shapes are often selected for dynamic studies because they show the adsorbent selectivity to the adsorbate of interest.

In cases, where regeneration is required because it may be related to an unfavorable isotherm , these isotherms are not useful [9].

The known Langmuir model provides good adjustments to strongly favorable isotherms as it forms a plateau that represents in many cases, the monolayer sorption.

Here, it must be remembered that the equilibrium equation is used in the modeling of fixed bed.

Below(Fig.2.1) are presented the adsorption isotherms.

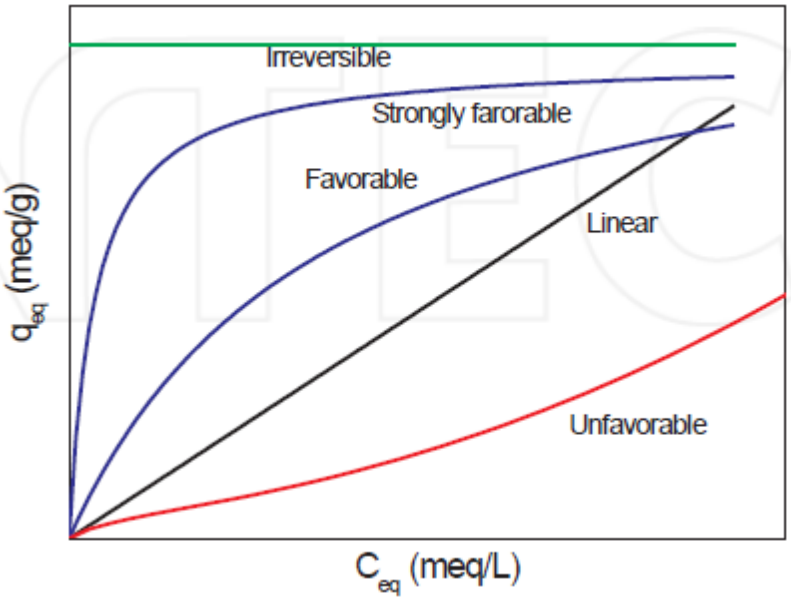

Figure 2.1. Adsorption isotherms [9]

The mathematical modeling has a key role in the scale up procedure from laboratory experiments through pilot plant to industrial scale. The adequate models can help to analyze and to explain experimental data, to identify mechanisms relevant to the process, to predict changes due to different operating conditions and to optimize the process overall productivity [9].

One should bear in his mind that the Langmuir isotherm is derived assuming a uniform surface, which is many cases is not valid. This relation works fairly well, even with adsorbents with high heterogeneity such as zeolites, clays or activated carbon [10].

In this point, some aspects about the Langmuir model should be stressed. The first one is related to the model itself. Sometimes the Langmuir model represents the experimental data although it is known that are different sites involved in the sorption

process such as the ones located in the supercages or in the sodalite cages of NaX zeolite [8].

On the other hand, the adsorbent may have high heterogeneity and only one type of site would be effective in the adsorption process.

In this case, the experimental data may be fitted successfully to such model and the assumptions previously considered are still valid. This may be the case of adsorption of large molecules such as **dyes** [9,10].

The scarce case of the extremely favorable isotherm is the irreversible adsorption represented by a horizontal line, that means a constant amount of adsorbed compound. When the irreversible isotherm is obtained no regeneration is possible(chemisorption). When one designs such dynamic adsorption processes also takes into account the multicomponent effluent[9].

It means that studies of batch competitive systems should be relevant. Adsorbents that have affinity to different adsorbates may be less effective in removing the one of interest. It these cases, higher packed beds are required. The multicomponent equilibrium data are obtained considering the initial multicomponent solution.

For the Langmuir isotherm system, to many models have been proposed so far.

The Binary Langmuir Model assumes a homogeneous surface with respect to the energy of adsorption, no interaction between adsorbed species and that all adsorption sites are equally available to all adsorbed species.

The Noncompetitive Langmuir Model considers that the concentration of the adsorbate of interest in the adsorbent depends on the concentration of the respective species in the fluid phase only. In this case, monocomponent Langmuir can be applied for each one of the species in solution [11].

In both cases, the Binary Langmuir Model and the Noncompetitive Langmuir Model, as there is no competition to the same sites, no overshooting is observed in the breakthrough curve.

The Langmuir Type Model was developed to describe the noncompetitive inhibition during enzymatic kinetic studies. According to the adsorption point of view such model may be applied when a synergism effect is presented due to the existence of sites containing both species [11].

It means that in the dynamic sorption more adsorption occurs than the one it was expected, and the uptake on the sorbate of interest is promoted by the presence of other sorbates. No overshooting is expected to occur in this system.

Myers and Prausnitz [12] developed the ideal adsorbed solution theory (IAST) based on the Gibbs adsorption isotherm.

The IAST model has the main advantage to predict the equilibrium in multicomponent systems in microporous materials through the single isotherms only. However, although the model allows its application in many complex mixtures of solutes, the IAST model limits its use in the range of concentration where the single equilibrium data were obtained. It has been used to predict the adsorption process in gas phase, mainly in diluted systems.

A non-predictive thermodynamic approach called RAST (Real Adsorbed Solution Theory) extends the IAST theory to more concentrated solutes using the corresponding activity coefficients.

Finally, when the ion exchange process is much more pronounced then the adsorption process, it may be applied the Ion Exchange Model taking into account the Mass Action Law. In typical ion exchangers such as zeolites this mode are applied with successful results.

After selecting the adsorbent and investigating the adsorption mechanism, the second step is the dynamic studies in the fixed-bed system.

2.2. Dynamic studies in fixed-bed systems

2.2.1. The breakthrough curve

Most adsorption and/or ion exchange operations, whether in laboratory or in plant-scale processes, are carried out in columns. A solution is passed through a bed of adsorbent beads where its composition is changed by adsorption [9].

The composition of the effluent and its change with time depend on the properties of the adsorbent (as already discussed), the composition of the feed, and the operating conditions (flow rate, temperature etc.).

Plots of the ratio C/Co (outlet adsorbate concentration/adsorbate feed concentration) versus time are called breakthrough curves [9].

As the run starts, most of the mass transfer takes place near the inlet of the bed, where the fluid first contacts the sorbent. If the solid contains no adsorbate at the start, the concentration in the fluid drops exponentially to zero before the end of the bed is reached.

This concentration profile as well as the breakthrough curve is shown in Figure 2.2. below.

As the run proceeds, the solid near the inlet is nearly saturated, and most of the mass transfer takes place further from the inlet. The concentration gradient is S shaped. The region where most of the change in concentration occurs is called the mass-transfer zone.

This is the real behavior of mass transfer process in fixed beds. When the axial or radial mass transfer resistances are neglected, adsorption occurs homogeneously and this is the ideal case. In fact, mass transfer resistances can be minimized but not effectively eliminated[9].

The limits of the breakthrough curve are often taken as C/Co values of 0.05 to 0.95, unless any other recommendation is fixed.

They are related to the breakpoint (t_b, C_b) and saturation point (t_s, C_s), respectively. In most of cases Cs =Co.

This is the case of wastewater treatment of highly toxic adsorbates. When the concentration reaches the limiting permissible value, say, 1 ppm, it is considered the break point.

The flow is stopped, the column is regenerated and the inlet concentration is redirected to a fresh sorbent bed [9].

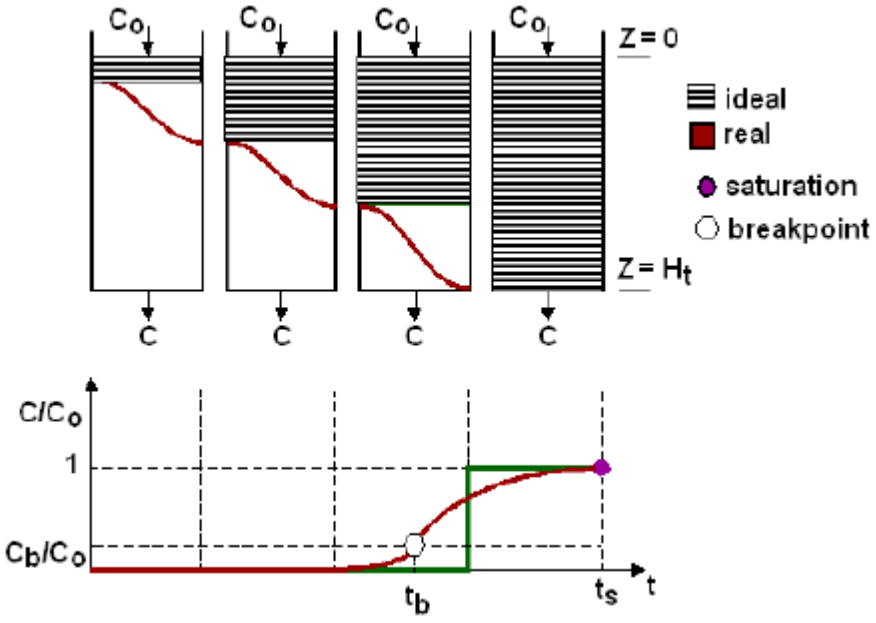

Figure 2.2. Breakthrough curve for the sorption process in fixed beds C_o is the concentration of the inlet solution, C_b is the concentration of the breakthrough, t_b is the breakpoint time and t_s is the saturation time [9].

2.2.2. Mass transfer in fixed-beds

In fixed-bed ion exchange, the concentration in the fluid phase and in the solid phase changes with time as well as with position in the bed. The transfer process is described by the overall volumetric coefficient (K_{ca}), obtained from a metal material balance in the column assuming irreversible sorption as proposed in McCabe et al.[9]:

$$K_c a = \frac{N \cdot u_o}{H_t} \qquad \text{(eq. 2.1)}$$

Where :

N= the overall number of transfer units

H_t= the bed length

u_o = the superficial velocity of the fluid

In fact, Eq. 2.1 can be used for modeling the breakthrough curves, if the batch isotherms can be considered as irreversible.

The overall number of transfer units may be obtained graphically by plotting C/Co versus N(τ-1), where N(τ-1) = 1+ln(C/Co) [9].

Parameter τ is dimensionless time defined as :

$$\tau = \frac{u_o C_o \left(t - \frac{\varepsilon}{u_o} H_t\right)}{\rho_p (1 - \varepsilon) W_{sat} H_t} \qquad \text{(eq. 2.2)}$$

The term $\frac{\varepsilon}{u_o} H_t$ in Eq. 2.2 is the time required to displace fluid from external voids in the bed, which is normally negligible. The product is the total amount of metal fed

per unit cross section of the bed up to time t and $\rho_p(1 - \varepsilon)W_{sat} H_t$ is the capacity of the bed, which is equal to the time equivalent to total stoichiometric capacity of the packed-bed tower (t_t) [9].

The time equivalent to usable capacity of the bed (t_u) and the time equivalent to total stoichiometric capacity of the packed-bed tower (t_t) if the entire bed reaches equilibrium are provided by a mass balance in the column and they are easily determined [13]:

$$t_u = \int_0^{t_b} \left(1 - \frac{C}{C_o}\right) dt \qquad \text{(eq.2.3)}$$

$$t_t = \int_0^{\infty} \left(1 - \frac{C}{C_o}\right) dt \qquad \text{(eq.2.4)}$$

where t_b is the breakpoint time.

If time t is assumed to be the time equivalent to the usable capacity of the bed (tu) up to t_b, parameter τ may be simplified to t_u/t_t. This ratio is the fraction of total bed capacity or length utilized to the breakpoint. Hence, the length of unused bed (HUNB) is the unused fraction times the total length (H_t) [13].

$$H_{UNB} = \left(1 - \frac{t_u}{t_t}\right) H_t \qquad \text{(eq.2.5)}$$

H_{UNB} is assumed to be constant and, as a consequence, an important tool when scaling-up processes [8].Unfortunately it is not always true. A constant mass-transfer zone is valid for ideal adsorption systems associated with adsorbates of small molecular diameter and simple structures [14].

Changes in pH speciation through the column may also change the MTZ(mass-transfer zone)[15].

It probably happens because the rate at which the sorption zone travels through the bed decreases with bed height [14].

Therefore, it may be concluded that the hypothesis of a constant length of mass transfer zone for the same feed concentration can be acceptable depending on the variation of the bed height and specific adsorbates.

H_{UNB} represents the mass-transfer zone (MTZ). Small values of this parameter mean that the breakthrough curve is close to an ideal step with negligible mass-transfer resistance. Moreover, in the ideal condition, no axial dispersion would occur.[14]. The velocity profile would be analogous to the one observed in a Plug Flow Reactor and the ideal breakthrough curve would be the response to a positive-step test, called the Cumulative Distribution Function or F curve.

In the ideal breakthrough curve H_{UNB} is zero. This condition is never reached although it is recommended to operate the column as close as possible. The closer the column is operated to the ideal condition, the more efficient is the mass transfer zone. Therefore, the ideal situation means $H_{UNB} = 0$.

In experimentally effective situation $0 < H_{UNB} < H_t$. If $H_{UNB} > H_t$ in the very beginning of the run the adsorbate is presented in the outlet solution, the sorption process is highly inefficient, mainly if the sorption unit has been used for wastewater treatment. An increase in H_t is recommended[14].

One of this parameter is the residence-time distribution (RTD). According to Fogler (2004), the RTD is determined experimentally by injecting a tracer in the column at some time t=0 and then measuring the outlet concentration as a function of time. In this case, the tracer is used to determine RTD in reactors and must be nonreactive, easily detectable, completely soluble to the mixture and more important: it should not adsorb on the walls or any other surface of the reactor [16].

If the injection of a tracer is given as a step injection, the response is the F curve which shape is analogous to the breakthrough curve as seen in Figure 2.2.

Then, it is possible to obtain the average residence time (t_{res}). Correlation between the F curve from the non-ideal concept and the sorption process in fixed beds can be done only in terms of the graphical shape. No more similarities are corrected.

The average residence time (t_{res}) of the fluid in the columnis estimated based on principles of probability as follows (Hill, 1977) [17]:

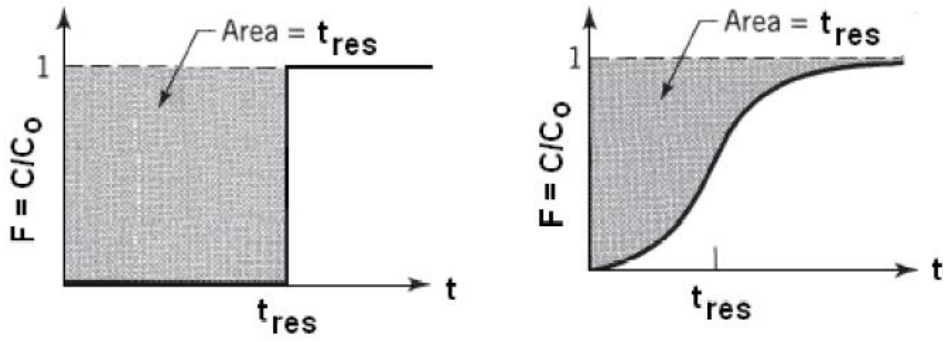

Figure 2.3. Breakthrough curves considering the F response of a step input: a) ideal situation ($H_{UNB} = 0$) b) real situation ($H_{UNB} > 0$).[17].

$$t_{res} = \int_0^{\infty} t dF(t)$$

(eq. 2.6)

where :

F(t) = the weight fraction of the effluent of an age less than t, which is equivalent to C/Co for breakthrough curves [18].

An indirect measure of how far from the optimum operational condition the column operates is expressed by the operational ratio (R) as [18].

$$R = \left| \frac{t_{res} - t_u}{t_u} \right|$$

(eq. 2.7)

Values of parameter R close to zero indicate that the operational conditions imposed are near the ideal condition, i.e., the optimal region of operation. Therefore, this difference may contribute to the selection of the best operational conditions in the column design [18].

With the average residence time it is also possible to evaluate the variance in the breakthrough curve [17]. which is given by:

$$\sigma^2 = \int_0^\infty t^2 \left(\frac{F(t)}{dt}\right) - t_{res}^2$$

(eq. 2.8)

The dimensionless variance should be calculated as :

$$\sigma_\theta^2 = \frac{\sigma^2}{t_{res}^2}$$

(eq.2.9)

Determination of this parameter is useful to estimate the axial dispersion in the packed bed.

Values of dimensionless variance close to zero mean that the behavior of the velocity profile in packed beds is close ideal plug-flow with negligible axial dispersion.

Finally, through a mass balance it is possible to obtain the amount of adsorbate retained up to the breakpoint time (U^{tb}) and up to the saturation time (U^{ts}) [17].

$$U^{t_b} = t_u . f_R . C_o$$

(eq.2.10)

$$U^{t_s} = t_t . f_R . C_o$$

(eq.2.11)

Where :

t_u and t_t are obtained through Eqs.2.3 and 2.4, f_R is the flow rate and Co is the inlet concentration.

2.2.3. Minimum mass transfer resistances in the fixed-bed system

Operate the fixed bed with minimum mass transfer resistances is quite advantageous. It maximizes the sorption process as more sorption sites are available to the dynamic process. Therefore, optimizing the operational conditions is highly recommended. It can be done investigating a range of particle diameters of the sorbent or different flow rates in the column [17].

In some cases, temperature should be also investigated. It is expected to obtain higher amount of uptaken sorbate with increasing temperatures when chemisorption and/or ion exchange are presented as the more significant mechanism. Nevertheless, if the retention is due to physisorption phenomenon, an increase in temperature is disadvantageous.

The optimal operational condition is the one that minimizes, as close as possible, the film and particle resistances, that means to maximize the pore diffusion and the solid diffusion.

Figure 2.3 gives an idea about the mass transfer mechanism in a fixed bed. Therefore, when the film and particle resistances are minimized it is seen that[17]:

The mass transfer zone, the operational ratio and the dimensionless variance are minimum.

The closer the system is of the optimal condition, the closer the breakpoint time is to the saturation time.

The adsorbate uptake up to breakpoint time (U^{tb}) and up to saturation time (U^{ts}) are the maximum[17].

It happens when there is at least a favorable isotherm; In most of cases, a steep breakthrough curve is observed.

Figure 2.4 shows an example of breakthrough curves at different flow rates. It is seen that at 11 mL/min the breakthrough curve is almost a step curve [17].

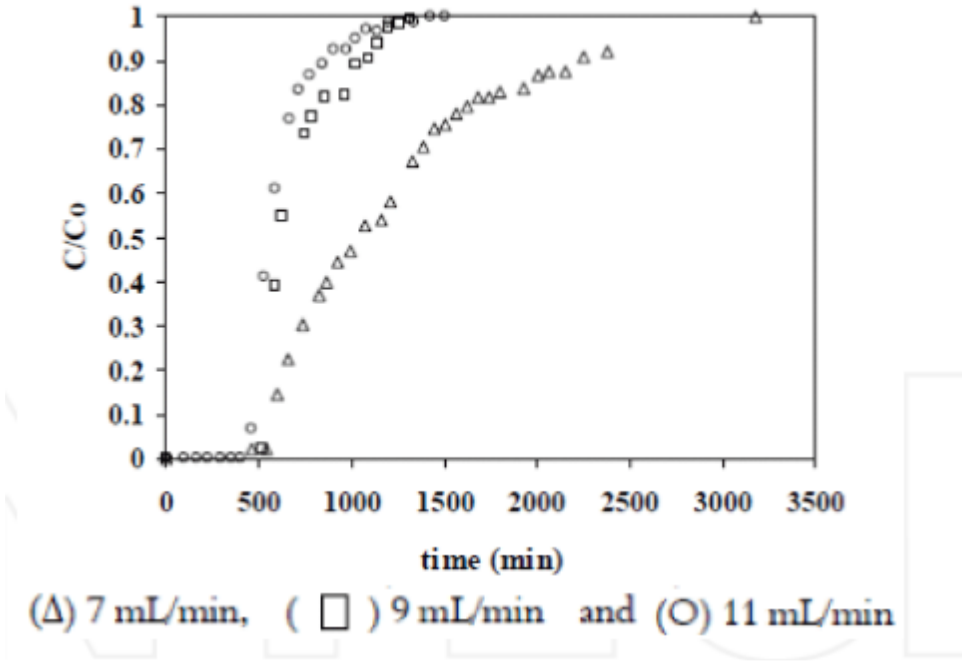

Figure 2.4. Breakthrough curves for Cr (III) uptake in NaA zeolite [18].

2.2.4. Adsorption in competing systems

When the feed solution is composed by different adsorbates, the competition for the adsorption sites may occur. Uptake of the adsorbate of interest is well evidenced by the dynamic capacity of the column [17].

Thus, the term $U^{tb}_{i\text{-}mix}$ is defined as the amount of adsorbate uptaken at t_b prior to the adsorbate i breakpoint [19].

The effect of competitive systems on the sorption process may be represented by the ratio of the uptake capacity for the adsorbent i in multicomponent solution and in single solution, that is the removal ratio $\left(U_{i\text{-}mix}^{t_b} \Big/ U_{i\text{-}single}^{t_b}\right)$ [20].

Thus if the removal ratio:

> 1: uptake is promoted by the presence of other adsorbates;

=1: no interaction exists between the adsorbates;

< 1: uptake is suppressed by the presence of other adsorbates.

Therefore, the evaluation of the removal ratio at the time equivalent to usable capacity of the bed t_u for sorbate i may be useful to investigate the influence of different sorbates on the uptake of such sorbate [7].

Moreover, in the competing systems, sometimes the breakthrough curves for the competing adsorbates may have values higher than one that is called overshooting. When the ion exchange phenomenon is dominant, it is also called sequential ion exchange .[7].

Figure 2.5 shows an example of a sequential ion exchange. The ion exchange preferentially occurs up to the occupation of all available sites. As the sorption proceeds, the competing sorbates are released at different running times with continued feed of the multicomponent solution [18].

Potassium ions are smaller than the other ions. Then, they diffuse faster into the ion exchanger framework and are firstly retained. Calcium ions are larger and probably face some difficulties in diffusing as fast as the potassium ions. Nevertheless, once they diffuse, they are preferentially retained due to its higher charge, displacing the potassium ions.

Finally, chromium ions are the largest ones with the highest charge. They diffuse slowly into the exchanger framework [18].

They displace the calcium ions. The consequence of such process is the presence of two overshooting waves: one related to the release of potassium ions and another related to the release of the calcium ions. In this competing ion exchange process it is seen that (U^{tb}_{Cr-mix} / $U^{tb}_{Cr-single}$) is 0.79, which means that there is a decrease of 21% in the chromium uptake. Probably the presence of potassium and mainly the presence of calcium ions suppressed the chromium uptake due to competition towards the exchanging sites located in the large cages of the zeolite NaY [18].

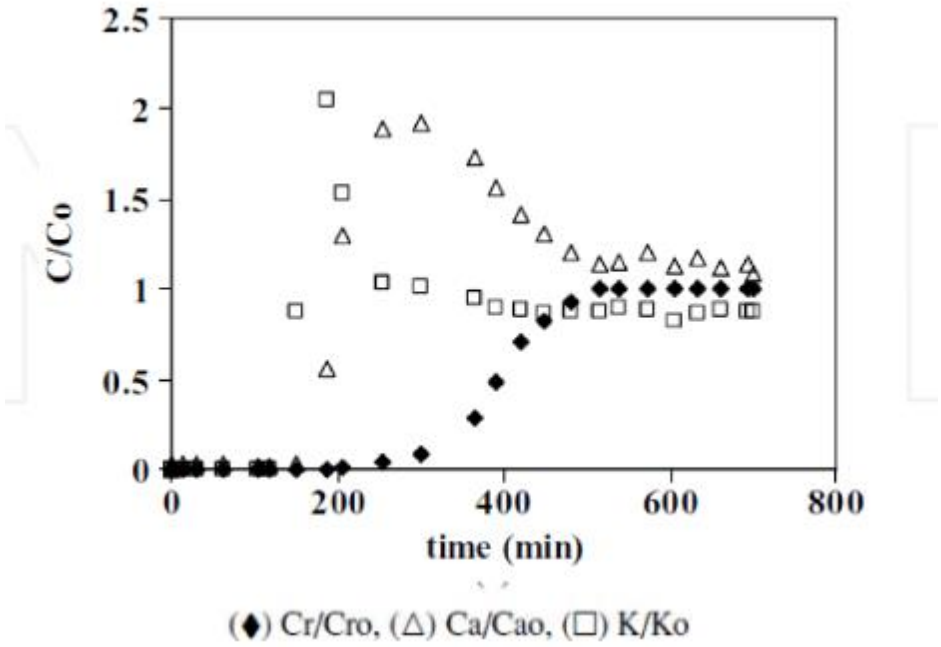

Figure 2.5: Breakthrough curves for competitive system Cr/Ca/K in NaY zeolite [18].

2.2.5. Dynamic isotherms

Most separation and purification processes that employ the sorption technology use continuous- flow columns. In order to understand and to model the dynamic process, a deep knowledge of the equilibrium in the fixed bed is essential [17].

For the complete comprehension of the whole process, information about the equilibrium and the kinetics of the process should be combined with the mass balance. Kinetic investigations in a column are almost exclusively restricted to those processes of which the equilibria either can be represented by a linear or a Langmuir isotherm or satisfy the law of mass action [17].

However, the results of this study of industrially applicable commercial products have shown that the above equilibria usually fail to fit the experimental results adequately. Furthermore, the customary procedures of determining the equilibria in batch systems are not, in general, applicable to all types of sorbents.[21].

For example, the batch isotherm was not able to represent correctly, the breakthrough curve of Cr (III) sorption in NaX zeolite modeled by a phenomenological model.

Figure 2.7 presents the batch isotherm of Cr (III) in zeolite NaX and its use in a LDF model. It is clearly seen that it is totally inadequate.

The dynamic isotherm surged to better describe the sorption mechanisms involved in a dynamic process where kinetics and equilibrium acts simultaneously. In fixed beds, solution is fed continuously, and, at equilibrium, concentration and pH are equal to their respective feed values that do not occur in batch isotherms. Its procedure is based on the breakthrough data.

Each run up to the saturation is related to one point of such data, that is, the amount of adsorbate retained up to saturation plotted against the inlet concentration [8].

The dynamic isotherm has the advantage of controlling the fluid-phase concentration. Results of the column dynamic simulations depend on the selection of an appropriate mathematical relation used to represent the equilibrium.

Therefore, in order to model the dynamic sorption, dynamic isotherms should be considered instead of the frequently used batch isotherms as they better represent equilibrium in fixed bed [22].

The dynamic isotherm of Cr (III) in NaX is shown in Figure 8 at the optimal particle size and flow rate previously determined [8]. Its shape is totally different, as one can see comparing Figures 2.8 and 2.7a.

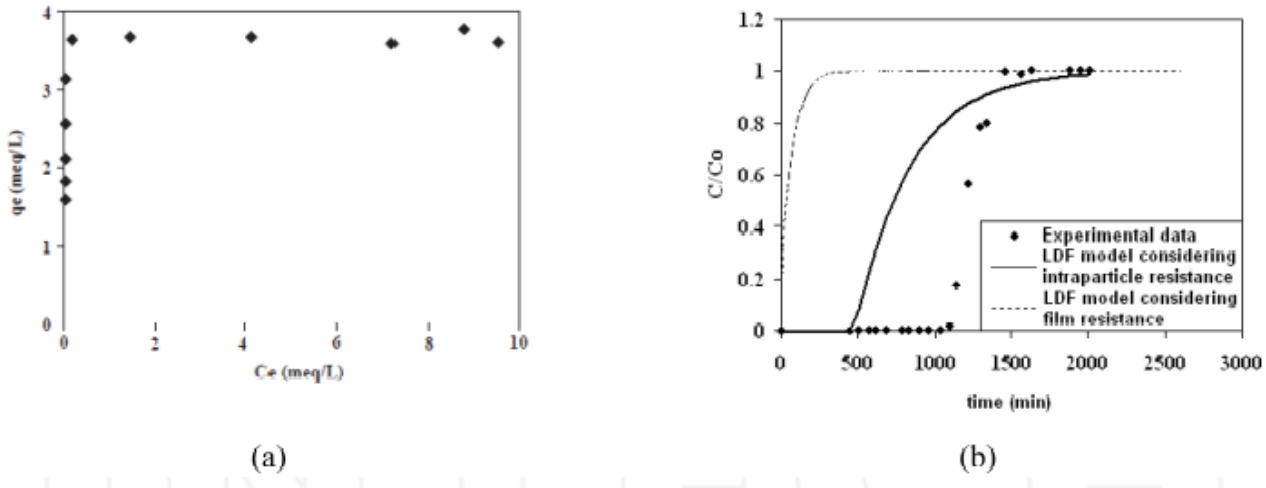

Figure 2.7. a) Batch isotherm of Cr (III) in zeolite NaX at 30 °C (b) Use of batch isotherm to model Cr (III) breakthrough data in NaX columns [8]

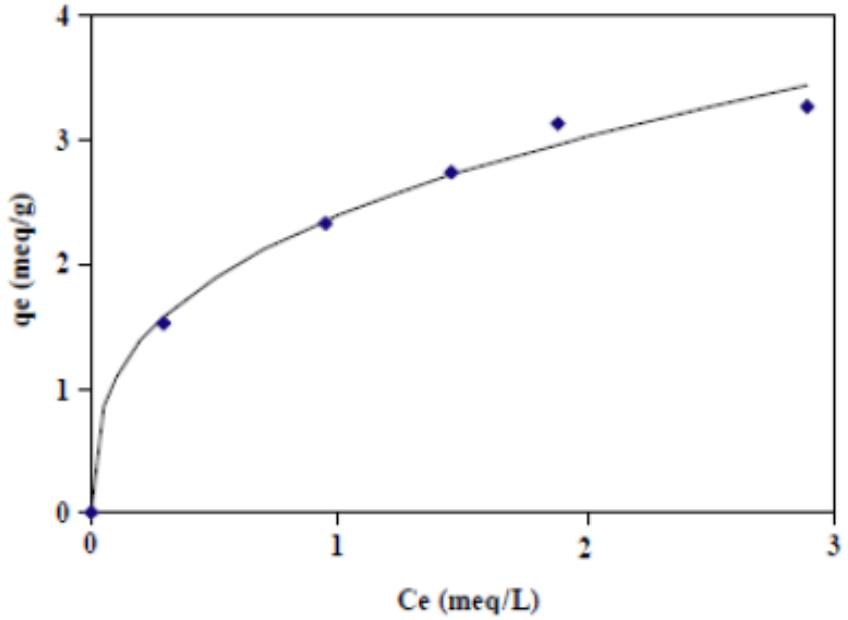

Figure 2.8. Dynamic isotherm of Cr (III) in zeolite NaX at 30 ^{0}C [8].

2.2.6. Modeling of the breakthrough curve

The phenomenological mathematical models are important tools in the design of adsorption in fixed bed columns. The validation is done by experimental data obtained in laboratory scale [17].

Mathematical models are useful for designing and optimizing purposes in industrial scale. expressed by non-linear mathematical equations. The concentration of the adsorbate varies with the position and time. Therefore, the phenomenological model is represented by partial differential equations, which are difficult to be solved analytically.

Due to such complexity, the phenomenological mathematical models have many simplifications to make them feasible to obtain an analytical solution.

Bohart and Adams (1920) developed one of the first mathematical models. The respective equation is given by equation 2.12.[23].

The model Bohart- Adams considers that the limiting step of the mass transfer is controlled by the kinetics of sorption which is represented by a second-order reaction.

$$\frac{C_{out}}{C^F} = \begin{cases} 0 & t < t_F \\ \dfrac{1}{\left(e^A + e^{-B} - 1\right)e^B} & t > t_F \end{cases}$$

(eq. 2.12)

where:

$$A = \frac{L\ \beta}{u_0},\ B = \frac{\left(-t u_0 + L\ \right)\beta}{\alpha u_0},\ \alpha = \frac{\rho_{bed} q^*}{C^F \varepsilon},\ \beta = k_a C^F \alpha \text{ and } t_F = \frac{L}{u_o}$$

Bohart and Adams model presented only one adjustable parameter that is the rate constant k_a. The parameter q*has been also reported as an adjustable parameter. However, its value can be determined is the saturation point of the breakthrough curves.

The model developed by Thomas (1944) has also analytical solution. The sorption rate is described by Langmuir adsorption kinetics. Both models, Thomas and Bohart and Adams consider negligible film and particle resistances as well as the dispersion within the column [24].

The Thomas mathematical model is obtained by mass balances of the sorbate in the fluid phase and in the solid phase. Such mass balances originate an equation that describe the equilibrium in the system. The mass balance in the fluid phase results in the following equation:

$$\frac{\partial C}{\partial t} + \rho_{bed}\frac{(1-\varepsilon)}{\varepsilon}\frac{\partial q}{\partial t} = -u_0\frac{\partial C_j}{\partial z} + D_L\frac{\partial^2 C_j}{\partial z^2}$$

(eq.2.13)

with the following initial and boundary conditions:

$C(0,z) = 0$ (eq.2.14)

In the inlet sample in the column (z = 0)[24]. :

$$D_L \frac{\partial C}{\partial z} = u_0 \left(C(t,0) - C^F \right)$$

(eq. 2.15)

In the outlet sample in the column(z = L):

$$\frac{\partial C}{\partial z} = 0$$

(eq. 2.16)

A rigorous mathematical model that takes into account the variation of the concentration of the adsorbate within the particle is described by the Fick's second law. In these cases, solution of equations of the bed and the particle should be solved simultaneously, which increases the complexity and computational effort. [24].

One alternative for reducing the computational effort is to replace Fick's Law by the simplified kinetics equation. The approach mostly used to replace the Fick's Law is the **LDF** model **(Linear Driving Force).** [25].

It applies the expression of the first order kinetics represented by Equation (2.17). Several authors have used such models with successful results for sorbents and biosorbents.

$$\frac{\partial q}{\partial t} = -K_S \left(q - q_{eq} \right)$$

(eq.2.17)

In the adsorption models represented by equation (2.17), it is assumed that the driving force for mass transfer is linear with the concentration of the sorbate in the solid. Moreover, it means the equilibrium condition at the interface between the local phase fluid, as illustrated in Figure 2.9.

The equilibrium in the adsorption process is usually represented by adsorption isotherms, such as: Langmuir, Freundlich, Tóth, Sips. Figure 2.9 also illustrates the mechanism of the external mass transfer occurs around the surface of the particle. From the interface solid- fluid, the mass transfer occurs, which is represented by following equation:

$$-K_S\left(q-q^*\right)=\frac{K_F a\varepsilon}{\rho_{bed}}\left(C-C_{eq}\right)$$

(eq. 2.18)

The mathematical model that considers both mass transfer resistances (external and intraparticle) is called double resistance model. This model is composed by the set of equations (2.13)-(2.18). When the mass transfer in predominantly intraparticle, that is($C_{eq}\approx$ C), the equilibrium concentration of the adsorbate in the solid is directly related to the concentration in bulk phase. In cases where the mass transfer resistance is in the film, that is ($C_{eq}\approx$ C), the rate of adsorption can be expressed by the following below[25]:

$$\frac{\partial q}{\partial t}=\frac{K_F a\varepsilon}{\rho_{bed}}\left(C-C_{eq}\right)$$

(eq. 2.19)

When the operational condition is experimentally optimized, the film and intraparticle resistances\ of the sorption processes (adsorption, ion exchange or adsorption + ion exchange) are minimized in the experimental range investigated. It means that the film thickness is the thinnest one and there is no significant steric resistance of the adsorbate in the particle pores.

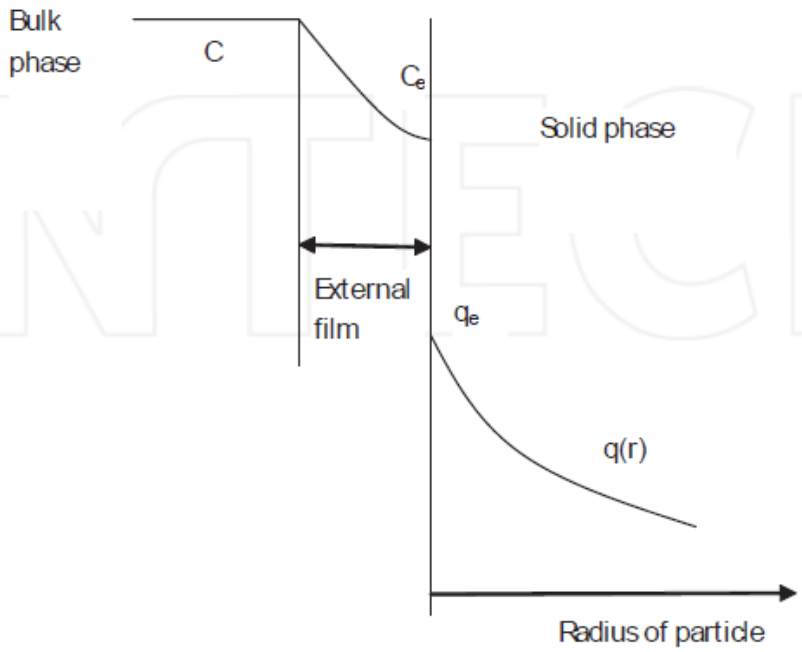

Figure 2.9. Mass transfer in adsorption process [25].

Some parameters of the model can be calculated from the correlation, namely: axial dispersion coefficient (DL) and external mass transfer coefficient. The relationship for calculating the axial dispersion is usually expressed from the dimensionless groups: Reynolds (Re), Peclet (Pe), Schmidt (Sc).

Delgado (2006) presents several correlations for calculating of axial dispersion of gases and liquids in packed beds. There are many correlations for calculating external mass transfer coefficients in porous media, usually expressed in terms of Reynolds (Rep), Schmidt and Sherwood (Shp) [26].

Delgado (2006) developed the following expression for 3<Rep<2000[26]:

$$Sh_p = 1 + 1.1\mathrm{Re}_p^{0.6} Sc^{1/3}$$

(eq. 2.20)

Where:

$$Sh_p = \frac{K_F d_p}{D}, \quad \mathrm{Re}_p = \frac{u_0 d_p}{\nu}, \quad Sc = \frac{\nu}{D}$$

The mass transfer coefficient in the solid (K_S) is an adjustable parameter of the model obtained from the experimental breakthrough curves.

Example – Modeling of breakthrough curves

Table 2.1 shows the experimental data of breakthrough curve of zinc in fixed bed columns using Na-Y zeolite as adsorbent obtained by Ostroski (2007) and Table 3 shows the operational conditions and bed parameters[27].

Table 2.1. Experimental data of zinc breakthrough curve

Time (min)	C_{out} / C^F
0.00	0.0000
22.00	0.0000
31.00	0.0000
55.00	0.0050
68.00	0.0156
74.00	0.1980
87.00	0.3564
93.00	0.5916
118.00	0.7721
136.00	0.8500
147.00	0.9248
180.00	0.9490
205.00	0.9655
230.00	0.9788
250.00	0.9874
260.00	0.9913
280.00	0.9963
307.00	1.0000

Table 2. 2. Operational conditions and bed parameters

C^F - Feed concentration of adsorbate (meq / cm³)	2.447x10^{-3}
L –Height of the bed (cm)	3.0
m_s - Weight of the adsorbent (g)	0.8
u_0 – Interstitial velocity (cm/min)	25.104
ε - Bed porosity	0.5
ρ_{bed} - Bed density (g / cm³)	0.4192

From these data it will be tested the Bohart and Adams and the LDF models that consider intraparticle resistance only. Both models have only one adjustable parameter: (k_a) for Bohart and Adams and (K_s) for LDF model.

Bohart and Adams model

From the experimental breakthrough curve it is calculated the capacity of the adsorbent (q*), since the column experiments are carried out up to the complete exhaustion of the column (saturation point), ie, when the concentration of sorbate in the outlet of the column is equal to the feed concentration. From a mass balance in the column, one can obtain the following equation:

$$q^* = \frac{C^F \dot{Q}}{1000 m_s} \int_0^{t_{END}} \left(1 - \frac{C_{out}}{C^F}\right) dt$$

(eq.2.21)

Where:

q * = Capacity of the adsorbent (meq/g)

C_{out} = Concentration of zinc in the outlet of the column (meq/L)

C^F = Feed concentration of zinc (meq/L)

$\dot{Q}$ = Volumetric flow rate (cm^3 /min)

t = time (min)

m_s = weight of adsorbent (g).

The capacity of the adsorbent was calculated from the area determinate by term

$\left(1-\frac{C_{out}}{C^F}\right)$ calculate by experimental breakthrough curve, illustrated in Figure 2.10.

The integral $\int_0^{t_{END}}\left(1-\frac{C_{out}}{C^F}\right)dt$ = 102.78min, calculated by trapeze method.

$$q^* = \frac{C^F \dot{Q}}{1000\, m_s}\int_0^{t_{END}}\left(1-\frac{C_{out}}{C^F}\right)dt = \left(\frac{2.447\times 8}{1000\times 0.8}\right)\times 102.78 = 2.515 \text{ meq/g}$$

$$\alpha = \frac{\rho_{bed} q^*}{C^F \varepsilon} = \left(\frac{0.4192\times 2.515}{2.447\times 10^{-3}\times 0.5}\right) = 861.7 \text{ meq/g}$$

$$\beta = k_a C_0 \alpha = k_a \times 861.7\times 10^{-3}\times 2.447 = 2.1086\, k_a$$

$$A = \frac{L\ \beta}{u_0} = \frac{0.8\times 2.1086 k_a}{25.104} = 67.20\, k_a$$

$$B = \frac{(-t u_0 + L\ )\beta}{\alpha\, u_0} = \frac{(-t\times 25.104 + 3)x2.1086\, k_a}{861.7\times 25.104} = 9.75\times 10^{-5}\times(3 - t\times 25.104)\, k_a \text{ min}$$

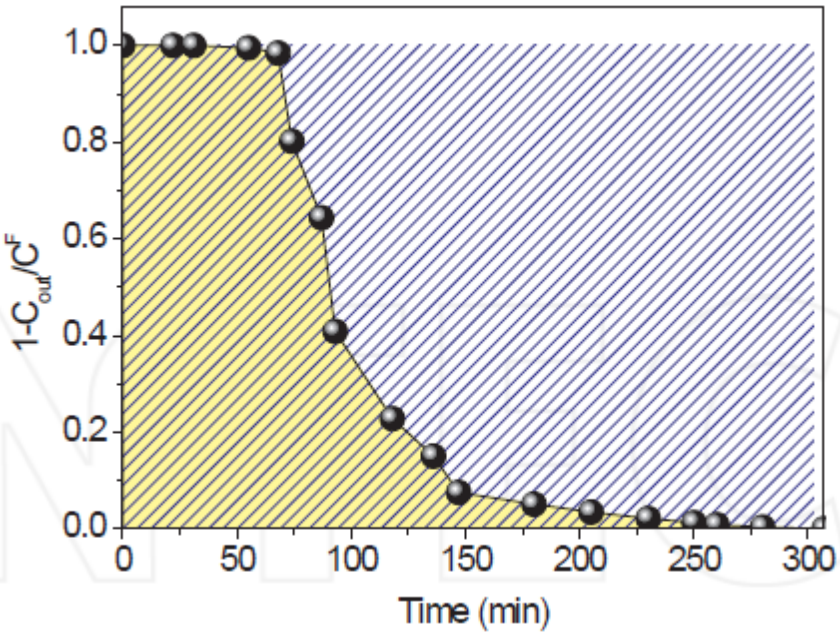

$\left(1-\frac{C_{out}}{C^F}\right)$

Figure 2.10. Area of curve

Applying in the equation (2.12), it follows that: $t_F = \frac{L}{u0} = \frac{0.8}{25.104} = 0.03187$

The parameter (k_a) estimated from the experimental data of breakthrough curve and applied method for one-dimensional optimization golden search, minimizing the following objective function:

$$F = \sum_{j=1}^{n_exp} \left(\left(\frac{C_{out}}{C^F} \right)_j^{EXP} - \left(\frac{C_{out}}{C^F} \right)_j^{EXP} \right)^2 \quad \text{(eq.2.22)}$$

Where:

$F = \sum_{j=1}^{n_exp} \left(\left(\frac{C_{out}}{C^F} \right)_j^{EXP} - \left(\frac{C_{out}}{C^F} \right)_j^{EXP} \right)^2$ = Ratio of the concentrations in the outlet of the column and feed determined experimentally

$\left(\frac{C_{out}}{C^F} \right)_j^{EXP}$ = Ratio of the concentrations in the outlet of the column and feed determined by model

$\left(\frac{C_{out}}{C^F} \right)_j^{MOD}$ = Number of experimental data

The value of adjustable parameter k_α was 22.35 (meq/cm^3.min)

CHAPTER 3 : THE ROLE OF MODELING IN SCALING UP THE FIXED-BED ADSORPTION COLUMN SYSTEMS

3.1. Introduction

Adsorption is a widely used method to treat industrial waste gas and effluent due to its low cost, high efficiency and easy operation.

Particularly, the adsorption process is suitable for decontaminating those compounds of low concentration or high toxicity, which are not readily treated by biological processes.

Based on the operation mode, adsorption can be generally classified into static adsorption and dynamic adsorption.

Static adsorption, also called batch adsorption, occurs in a closed system containing a desired amount of adsorbent contacting with a certain volume of adsorbate solution, while dynamic adsorption usually occurs in an open system where adsorbate solution continuously passes through a column packed with adsorbent.

For column adsorption, how to determine the breakthrough curve is a very important issue because it provides the basic but predominant information for the design of a column adsorption system.

Without the information of the breakthrough curve one cannot determine a rational scale of a column adsorption for practical application.

There are two widely used approaches to obtain the breakthrough curve of a given adsorption system: direct experimentation or mathematical modeling.

The experimental method could provide a direct and concise breakthrough curve of a given system.

However, it is usually a time-consuming and economical undesirable process, particularly for the trace contaminants and long residence time.

Also, it greatly depends upon the experimental conditions, such as ambient temperature and residence time.

Comparatively, mathematical modeling is simple and readily realized with no experimental apparatus required, and thus, it has attracted increasing interest in the past decades.

Currently, a variety of mathematical models have been used to describe and predict the breakthrough curves of a column adsorption system in liquid or gaseous phase but there is still lack of a comprehensive review of these models[28,29,30].

The main objective of the present review is to introduce the modeling of dynamic adsorption in liquid phase.

Different from the gas-solid adsorption, liquid-solid adsorption is more theoretically difficult to give an unambiguous description because the solvent accompanies more intricate interaction between the species involved.

Moreover, the salvation effect results in a more complicated behavior of the process. To model a liquid-solid column adsorption, it is necessary to divide it into four basic steps (Fig.3.1):

(1) liquid phase mass transfer including convective mass transfer and molecular diffusion

(2) interface diffusion between liquid phase and the exterior surface of the adsorbent (i.e., film diffusion)

(3) intrapellet mass transfer involving pore diffusion and surface diffusion; and, (4) the adsorption- desorption reactio[31,32].

(1) Liquid phase mass transfer. Molecules or ions in the column can move in both axial and radial directions. For simplification, it is common to postulate that all cross-sections are homogeneous and the radial movement could be neglected. Thus, a macroscopic mass conservation equation is acquired to represent the relationship between the corresponding variations (i.e., concentration of the adsorbed adsorbate q; concentration of the bulk solution C; distance to the inlet z; superficial velocity u; and axial dispersion coefficient Dz (if the axial dispersion is not ignored).

Regarding a control volume as shown in Fig.3. 2, one has to use the equation[33] :

$$\varepsilon \frac{\partial C}{\partial t} + u \frac{\partial C}{\partial z} + (1-\varepsilon)\rho_a \frac{\partial q}{\partial t} = D_z \frac{\partial^2 C}{\partial z^2},$$

(eq 3.1)

where initial and boundary conditions are :

$$t = 0 \rightarrow C(z,t) = 0,$$
$$t = 0 \rightarrow q(z,t) = 0,$$
$$z = 0 \rightarrow C(0,t = 0) = 0,\ C(0,t > 0) = C_{\mathrm{F}},$$
$$z = H \rightarrow \frac{\partial C}{\partial z} = 0.$$

When the axial dispersion is ignored,[33]

$$\varepsilon \frac{\partial C}{\partial t} + u \frac{\partial C}{\partial z} + (1-\varepsilon)\rho_{\mathrm{a}} \frac{\partial q}{\partial t} = 0.$$

(eq. 3.2)

The initial and boundary conditions turn to:

$$t = 0 \rightarrow C(z,t) = 0,$$
$$z = 0 \rightarrow C = C_{\mathrm{F}} + \frac{D_z \varepsilon}{u} \frac{\partial C}{\partial z},$$
$$z = H \rightarrow \frac{\partial C}{\partial z} = 0,$$

where :

ε = the bed porosity

t = the time,

ρ_a = the adsorbent density

C_F = the initial concentration of the influent and

H = the bed height. [33].

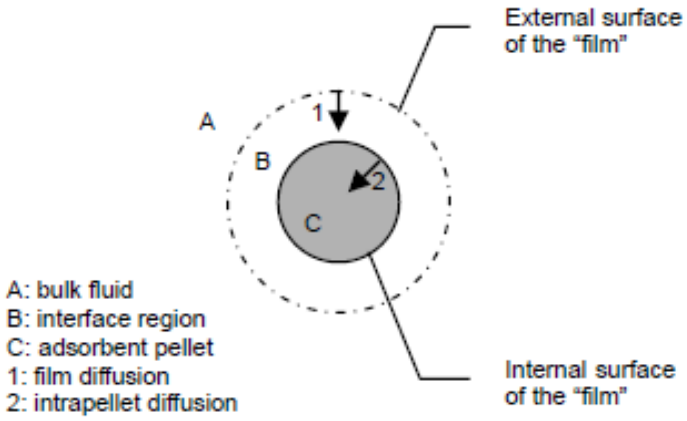

Figure 3.1.Macroscopic adsorption process of an adsorbent pellet [33]

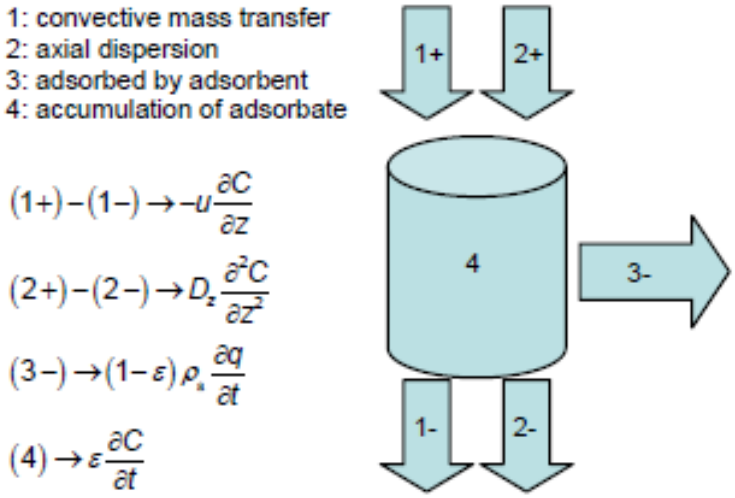

Figure 3.2. Schematic diagram of the mass conservation of a control volume [33]

Eqs. (3.1) and (3.2) are based on the following assumptions:

(1) the process is isothermal

(2) no chemical reaction occurs in the column

(3) the packing material is made of porous particles that are spherical and uniform in size

(4) the bed is homogenous and the concentration gradient in the radial direction of the bed is negligible

(5) the flow rate is constant and invariant with the column position and,

(6) the activity coefficient of each species is unity [34].

(2) Film diffusion. The driving force of film diffusion is the concentration gradient located at the interface region between the exterior surface of adsorbent pellets and the bulk solution. As the first step of adsorption, film diffusion predominates the overall uptake rate to some extent and even becomes the rate control step in some cases. The flux film diffusion can be expressed in linear form by multiplying its driving force and the phenomenological coefficient [33]

$$\frac{dq}{dt} = J_f = k_f a(C - C_s), \qquad \text{(eq. 3.3)}$$

Where :

J_f = the mass transfer flux

α= the volumetric surface area,

Cs = the adsorbate concentration at the exterior surface of adsorbent, and

k_f = the film diffusion coefficient.

It is generally known that increasing the flow rate will decrease the film thickness and resistance, whereas larger film resistance can be caused by packing with smaller adsorbent pellets due to the extension of the exterior surface area.

(3) Intrapellet diffusion and reaction. As shown in Fig.3. 3, surface diffusion and pore diffusion proceed in parallel accompanying with Knudsen diffusion and the adsorption reactions.

Of note, when the pore size is only slightly larger than the diameter of adsorbate ions or molecules, the Knudsen diffusion begins to play a significant role as shown in Fig. 3.3b.

Generally speaking, the film diffusion driven solely by the concentration gradient can be expressed in a routine form (Eq. (3.3), and the intrapellet diffusion, which is more complex and diverse, is the keystone of modeling dynamic adsorption.

Pore diffusion, surface diffusion and reaction are involved in intrapellet transfer simultaneously, and a set of equations could be set to consider all the possible mechanisms[33].

Moreover, consideration of the heterogeneity and Knudsen diffusion will tend to cause dramatic complexity and make the process very tedious.

Hence, it is urgent to simplify such a process by making appropriate assumptions based on specific characteristics of the system, and several models were proposed based on different simplifications indeed[33]

Most mathematical models to predict a breakthrough curve have (or are acquired by) the same composition, i.e., (a) macroscopic mass conservation equation

(b) adsorption kinetic equation (sometimes including a set of equations) and

(c) equilibrium relationship.

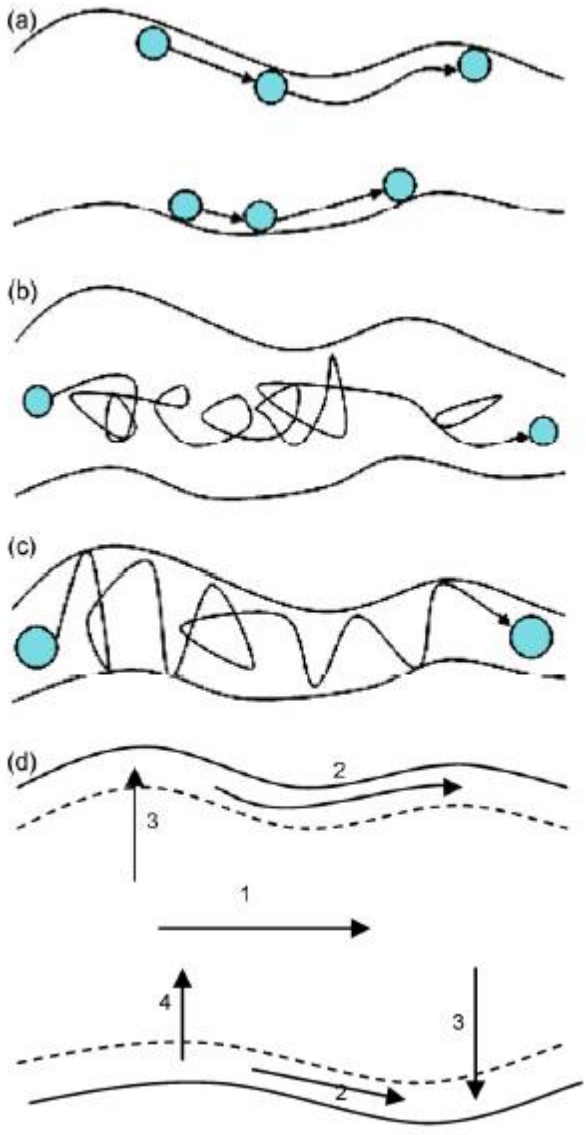

Figure 3.3. Macroscopic schematic illustration of basic diffusion and adsorption steps inside the pore (a) Surface diffusion; (b) Pore diffusion; (c) Pore diffusion with

significant Knudsen diffusion; (d) Combination of intrapellet diffusion and adsorption. 1: pore diffusion; 2: surface
diffusion; 3: adsorption; 4: desorption [33]

3.2. Single-component isotherms

As we have illustrated, the general way to predict the breakthrough curve is to solve a set of partial differential equations which consist of a macroscopic mass conservation equation, uptake rate equation (sometimes including a set of equations), and isotherm equation.

Obviously, as a prerequisite of modeling of the dynamic adsorption, the choice of the isotherm style will directly affect the effect of mathematic modeling. Although several methods have been adopted to determine the isotherm, the most widely used one is the conventional static method proceeding in a closed system. Actually, due to the complexity of the structure of adsorbent and the interaction between each corpuscle, isotherms can present diverse shapes.

Malek and Farooq (1996) suggested that there are three fundamental means to formulate an isotherm: dynamic equilibrium between adsorption and desorption, thermodynamic equilibrium between phases and species, and adsorption potential theory [35].

Although researchers have developed various isotherm models in the past decades, it is clear that none of them fit well with all cases, and thus, one has to determine the best suitable isotherm experimentally.

Medved, I,and Cerny, R., (2011), reviewed the means to derive the isotherm by both batch method and adsorption-desorption method [36].

Here we do not intend to give a detailed discussion of various isotherms but only concisely introduce several widespread models.

3.2.1. Langmuir isotherm

The Langmuir isotherm assumes:

(1) the adsorption process takes place as monolayer adsorption (chemical adsorption);

(2) the surface of adsorbent pellets or each adsorption site is homogeneous; and,

(3) the adsorption heat does not vary with the coverage.

In other words, in terms of the Langmuir isotherm, adsorption takes place when a free adsorbate molecule collides with an unoccupied adsorption site and each adsorbed molecule has the same percentage to desorption [37]. The model can be written as:

$$q_e = \frac{q_m b C_e}{1 + b C_e},$$

(eq. 3.4)

Where :

q_e = the value of q at equilibrium,

q_m = the maximum adsorptive capacity,

Ce= the concentration of adsorbate in liquid phase at equilibrium, and

b = the Langmuir constant.

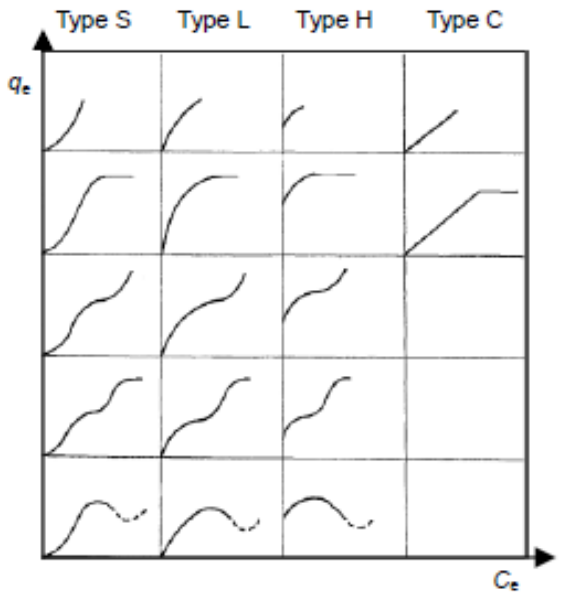

Figure 3.4. Adsorption isotherms [38].

Certainly, we can obtain a linear form of the Langmuir model :

$$\frac{C_e}{q_e} = \frac{1}{q_m b} + \frac{C_e}{q_m},$$

(eq. 3.5)

Where :

$$b = k_a / k_d,$$

(eq. 3.6)

Where :

k_a = the adsorption rate coefficient of the Langmuir kinetic model, and

k_d = the desorption rate coefficient [39].

Despite the reversible adsorption nature of the Langmuir model, it sometimes fits irreversible adsorption well. Because of its simple form and well fitting performance, the Langmuir isotherm has become one of the most popular models in adsorption studies.

3.2.2. Freundlich isotherm

Another most widely used model is the Freundlich isotherm. Comparing with the Langmuir isotherm, the Freundlich isotherm does not have much limitation, i.e., it can deal with both homogeneous and heterogeneous surfaces, and both physical and chemical adsorption.

Especially, this model frequently succeeds in depicting the adsorption behavior of organic compounds and reactive matters. The Freundlich isotherm is expressed as

$$q_e = K C_e^{1/n}$$

(eq. 3.7)

and its linear form is

$$\ln q_e = \ln K + \frac{1}{n} \ln C_e$$

(eq. 3.8)

where K and n are the parameters to be determined.

Though the Freundlich isotherm is one of the earliest empirical correlation, it could be deduced from the assumption that $Qa=Qa,_0–a_f \ln\theta$, where Qa is the differential heat of adsorption, θ is the coverage, $Qa,_0$ is the value of Qa at θ=0, and a_f is a constant. According to (Haghseresht and Lu, 1998), the surface heterogeneity and type of adsorption can be roughly estimated by the Freundlich parameters [40].

3.4. Modeling of fixed-bed adsorption

As one of the most prevalent techniques for separation and purification, fixed-bed adsorption has been widely applied for its high efficiency and easy operation.

How to optimize the design and operation conditions of the fixed-bed adsorption is obviously an important issue to be focused on [40].

Given the fact that experimental determination of the adsorption performance under diverse conditions is usually expensive and time-consuming, development of mathematical models to predict fixed-bed adsorption is necessary.

An ideal model should be mathematically convenient, be able to give an exact estimation of the breakthrough behavior, and evaluate the effect of each variable on adsorption.

A dynamic adsorption model usually consists of a macroscopic mass conservation equation, uptake rate equation(s) and isotherm. Considering the different components of the adsorption systems (solvents, adsorbate, adsorbent), variable operation conditions and specific demands of accuracy and calculative simplicity, it is an important but challenging task to propose a general use model, because most models derived from different assumptions are only suitable for a limited situation but fail to describe others.

3.4.1. General rate models

Based on the assumption that the rate of intrapellet diffusion is described by Fick's Law, some different expressions of general rate models were developed, such as the pore diffusion model (PDM), homogeneous surface diffusion model (HSDM), and pore and surface diffusion model (PSDM).PDM can be described as (Du et al., 2008)[41]. :

$$\varepsilon\frac{\partial C}{\partial t}+\rho\frac{\partial q}{\partial t}=\frac{\rho D_{ep}}{r^2}\frac{\partial}{\partial r}\left(r^2\frac{\partial q}{\partial r}\right)$$

(eq. 3.9)

with the initial and boundary conditions as :

$$0\le z\le H, 0\le r\le r_p, t=0\rightarrow q=0,$$

$$r=0\rightarrow\frac{\partial q}{\partial r}=0,$$

$$r=r_p\rightarrow D_{ep}\left(\frac{\partial q}{\partial r}\right)_{r=r_p}=k_f a(C-C_s),$$

(eq. 3.10)

Where :

ρ = the bed density

r_p = the radius of adsorbentpellets

D_{ep} = the effective pore diffusion coefficient and

r = the distance to the centre of the pellet

The basic mathematic form of HSDM is [42] :

$$\varepsilon\frac{\partial C}{\partial t}+\rho\frac{\partial q}{\partial t}=\frac{D_s}{r^2}\frac{\partial}{\partial r}\left(r^2\frac{\partial q}{\partial r}\right)$$

(eq. 3.11)

with its initial and boundary conditions as :

$$0\le z\le H, 0\le r\le r_p, t=0\rightarrow q=0,$$

$$r=0\rightarrow\frac{\partial q}{\partial r}=0,$$

$$r=r_p\rightarrow \rho D_s\left(\frac{\partial q}{\partial r}\right)_{r=r_p}=k_f a(C-C_s),$$

(eq. 3.12)

where Ds is the surface diffusion coefficient.

In addition, PSDM can be represented as (Liu et al., 2010)[43] :

$$\varepsilon \frac{\partial C}{\partial t} + \rho \frac{\partial q}{\partial t} = \frac{D_s}{r^2} \frac{\partial}{\partial r}\left(r^2 \frac{\partial q}{\partial r} \right) + \frac{\rho D_{ep}}{r^2} \left(r^2 \frac{\partial q}{\partial r} \right).$$

(eq. 3.13)

with its specific initial and boundary conditions of :

$$0 \le z \le H, 0 \le r \le r_p, t = 0 \rightarrow q = 0,$$

$$r = 0 \rightarrow \frac{\partial q}{\partial r} = 0,$$

$$r = r_p \rightarrow \left[\left(D_{ep} + D_s \rho \frac{dq}{dC} \right) \frac{\partial C}{\partial r} \right]_{r=r_p} = k_f a (C - C_s).$$

Due to the fact that $\rho \frac{\partial q}{\partial t}$ is usually much higher than $\varepsilon \frac{\partial C}{\partial t}$, the latter term was neglected in most cases.

With distinct rate control step(s) of different systems, the appropriate type of the general rate models should be applied, including the film-pore diffusion model, film-surface diffusion model and film-pore/surface diffusion model.

Reasonably, the film diffusion can be neglected when the film mass transfer resistance is quite small (i.e., negligible concentration gradient in the film).

However, additional experiments should be performed to ensure that film diffusion is not a rate control step.

Note that among Eqs. (3.9)–(3.11), the term of the surface reaction rate is not involved in most cases because it is much faster than other diffusion steps. Sometimes the surface reaction should be considered when it significantly affects the total adsorption rate or even becomes the sole rate control step.

Plazinski et al. (2009) made a comprehensive review of sorption kinetics including surface reaction mechanism [44].

When a proper liquid phase continuity equation (eq. (3.1) or (3.2)), film diffusion equation (eq. (3.3)), intrapellet diffusion equation, and isotherm equation are available, it is possible to generate the breakthrough curve by solving these partial differential equations.

Note that several parameters in the general rate models can be determined both theoretically and experimentally.

Especially, to our knowledge, there is no reliable method to theoretically predict the tortuosity τ and surface diffusion coefficient Ds, which are indispensable when using the general rate models.

Thus, for trustworthy prediction, it is inevitable to use the experimental method to determinate these parameters.

To directly solve the general rate models is usually a time-consuming and computationally troubled work.

A review of surface diffusion is available elsewhere (Medved and Cerny, 2011),which might provide some ideas to modify the intrapellet diffusion models[36].

The prevalence of the conventional/modified general rate models is not only because they give good prediction of dynamic adsorption, but also involves

a variety of parameters to determine the process variables.

The variables could be optimized by keeping other parameters constant and comparing the breakthrough curves predicted by this model under different values of the target parameter "*X*", for example, 0.5*X*, *X* and 2*X* (Note that adjusting a parameter may lead to variation in the phenomenological coefficient(s), and optimization based on modeling is not a precise method).

However, the main limitation of these models is the complicated and time-consuming computation.

3.4.2. Linear driving force (LDF) model

The linear driving force (LDF) model proposed by (Glueckauf, 1955) formulates a lumped mass transfer coefficient to represent the intrapellet diffusion rate, as written in a linear form as[45] :

$$\frac{dq}{dt} = k_e(q_s - q_a) \quad \text{(eq. 3.14)}$$

Where :

q_a = the average concentration of the adsorbed adsorbate

q_s = the loading of the adsorbate at the external surface of adsorbent, and

k_e = the lump intrapellet diffusion kinetic coefficient

The original LDF model regards that qs in equilibrium corresponds to the concentration of the bulk solution C. In other words, it neglected the concentration gradient in the interface region between the liquid phase and adsorbent, and k_e is a function of intrapellet diffusivity.

When the mass transfer within the interface is involved, the film diffusion equation should be added into the LDF model, namely

$$\frac{dq}{dt} = k_f a(C - C_s).$$

(eq. 3.15)

Combining Eqs. (3.14) and (3.15) with the liquid phase mass conservation equation and proper isotherm, it is possible to predict the breakthrough curve. Hence, the LDF model can be used to estimate the coefficients k_e and k_f.

Similar to the general rate models, these parameters can be acquired by the theoretical and experimental ways. For the theoretical way, a widely accepted expression is written as [45]:

$$k_e = \frac{15D_e}{r_p^2}.$$

(eq. 3.16)

When intrapellet diffusion is dominated by pore diffusion :

$$k_e = \frac{15D_p}{f'(C)\rho r_p^2}.$$

(eq. 3.17)

While by surface diffusion :

$$k_e = \frac{15 D_s}{r_p^2}.$$

(eq. 3.18)

An empirical equation of the rate constant was developed previously[46]:

$$k_e = 0.00129\left[D_M C_F / \left(r_p^2 q_F \right) \right]^{1/2}$$

(eq. 3.19)

where :

De = the effective intrapellet diffusion coefficient involving both surface diffusion and pore diffusion and f′(C) is related to the isotherm. Except for Ds and De, all the parameters are available by directly measuring or referring to the corresponding isotherms.

Note that $\frac{dq}{dc}$ is not constant if the isotherm is nonlinear (i.e., does not obey Henry's Law). Hence, to obtain the value of De, an average value has to be applied to represent f′(C). As for Ds, it can be reckoned by combining eqs. (3.18) and (3.19):

$$\frac{15 D_s}{r_p^2} = 0.00129\left[D_M C_F / \left(r_p^2 q_F \right) \right]^{1/2}$$

(eq. 3.20)

and then calculate De by :

$$D_e = D_s + D_p / \left(f'(C) \rho \right).$$

(eq. 3.21)

The calculated kinetic parameters sometimes fit well with the experimental data, but conspicuous deviation may appear in other cases. For instance, the theoretical value is often much higher than the experimental result when the dissolved organic matter (DOM) is adsorbed. In that case, the theoretical method could just approximately

reckon the adsorption performance, and the parameters have to be determined by the experimental breakthrough curves.

Another expression of the LDF model is available by incorporating eqs. (3.14) and (3.15):

$$\frac{\partial q}{\partial t} = k_o (q_s - q_a)$$

(eq.3.22)

Where :

k_o = the overall kinetic constant combining both the film diffusivity and the intrapellet diffusivity.

Additionally, surface reaction was also involved in LDF in some cases [47].

Computational software is often required to derive the numerical solution of the LDF model, especially when the isotherm is in the nonlinear form. Nevertheless, as compared to the general rate models, the LDF model could reduce the computational time significantly and its accuracy was generally acceptable.

Hence, the LDF model has become one of the most widely used models now. For some recent developments of the LDF model one could refer to the work by Gholami and Talaie (2010) [48].

3.4.3. Clark model

As is well known, granular active carbon (GAC) is one of the most popular adsorbents with micropore structure.

US EPA even initiated a series of field studies to evaluate the performance of GAC and acquired sufficient data.

Based on the data from US EPA, Clark (1987) developed a model to predict the performance of GAC-organic compounds adsorption system. The Clark model was deduced based on the following equations and assumption.[49].

(1) Liquid phase continuity equation is :

$$J = \frac{Q_A AC - Q_A A(C - \Delta C)}{A\Delta z}.$$

(eq. 3.23)

(2) The shape of the mass-transfer zone is constant and all the adsorbates are removed at the end of the column

$$Q_A C = u_a q_F.$$

(eq. 3.24)

(3) The isotherm fits the Freundlich type:

$$q_e = KC^{1/n}.$$

(eq. 3.25)

(4) Expression of the adsorption rate is :

$$J = Q_A \frac{dC}{dz} = K_T(C - C_e)$$

(eq. 3.26)

where :

J = the mass-transfer rate per unit reactor volume

A = the column cross-section area

Q_A = the volumetric flow rate per unit of cross-section area,

u_a = the mass velocity of the adsorbent to maintain the mass-transfer zone stationary,

ΔC = the incremental change of concentration, and

Δz = the differential reactor height.

The final expression of Clark model is :

$$\left(\frac{C_{in}^{n-1}}{1 + Be^{-r't}}\right)^{1/(n-1)} = C$$

(eq. 3.27)

$$B = \left(\frac{C_{in}^{n-1}}{C_b^{n-1}} - 1 \right) e^{r' t_b} \qquad \text{(eq. 3.28)}$$

$$r' = (n-1) \frac{K_T}{Q_a} \frac{dz}{dt} \qquad \text{(eq. 3.29)}$$

Where :

C_b = the breakthrough concentration

t_b = the service time, and

C_{in} =the constant influent value on the carbon bed.

The following procedures should be completed prior to using the model[49].

(1) Determine n by the batch experiment

(2) Rearrange Eq. (3.28) into :

$$\ln\left[\left(\frac{C_F}{C}\right)^{n-1} - 1\right] = -r't + \ln B. \qquad \text{(eq. 3.30)}$$

(3) The slope and intercept of the plot of $\ln[(C_F/C)^{1/n}-1]$ vs. t allow one to solve r' and B, respectively.

(4) Generate the whole breakthrough curve.

It is clear that the mass conservation equation in the column is different from those discussed above.

We find that eq. (3.26) actually disregards the accumulation of adsorbate concentration.

In other words, it does not reflect the time difference between C and C+ΔC. If taking a controlled volume V (the volume passing through any cross-section per unit time) into consideration and postulating the uniformity of the control volume and negligible molecular diffusion, we obtain [49]:

$$\varepsilon VC_{z,t} - \rho VJ\Delta t = \varepsilon VC_{z+\Delta z,t+\Delta t}.$$

(eq. 3.31)

When $\Delta t \rightarrow 0$, then :

$$\varepsilon VC_{z,t} - \rho VJ\mathrm{d}t = \varepsilon VC_{z+\mathrm{d}z,t+\mathrm{d}t}.$$

(eq. 3.32)

Additionally :

$$C_{z+\mathrm{d}z,t+\mathrm{d}t} = C_{z,t} + \frac{\partial C}{\partial z}\mathrm{d}z + \frac{\partial C}{\partial t}\mathrm{d}t.$$

(eq. 3.33)

Cancelling Vdt of eq. (3.32) and combining eq. (3.33) we have :

$$\rho J = -u_i \varepsilon \frac{\partial C}{\partial z} - \varepsilon \frac{\partial C}{\partial t}.$$

(eq. 3.34)

The same conclusion can also be made when assuming:

$$\rho_a (1-\varepsilon)\left(\frac{\partial q}{\partial t}\right) + u\left(\frac{\partial C}{\partial z}\right) >> \varepsilon\left(\frac{\partial C}{\partial t}\right).$$

However, the Clark model has successfully predicted a variety of systems and even those not following this assumption.

As mentioned above, the dynamic adsorption is such a complicated process that it is almost impossible to give a complete description of each variable.

Actually, even the "most theoretically rigorous" general rate models are still simplified from the real situations, such as the distribution of adsorbent pellets with different size in the column, the wall effect, the mass transfer caused by momentum transfer and heat transfer.

Moreover, by mathematical fitting, each phenomenological coefficient could be adjusted to the optimal values, which would compensate for the inherent shortages of the model to some extent.

Thus, it is still rational to suppose the Clark model has good performance under different conditions [49].

3.4.4. Thomas model

The Thomas model is another one frequently applied to estimate the adsorptive capacity of adsorbent and predict breakthrough curves, assuming the second-order reversible reaction kinetics and the Langmuir isotherm [50].

Theoretically, it is suitable to estimate the adsorption process where external and internal diffusion resistances are extremely small. [51].

The Thomas model is given by [24]:

$$\ln\left(\frac{C_F}{C}-1\right)=\frac{k_{Th}q_F m}{Q}-k_{Th}C_F t \qquad (3.35)$$

Where :

k_{Th} = the Thomas rate constant,

m = the mass of adsorbent in the column.

With several couples of m and Q, k_{Th} and q_F values derived through a plot of $\ln[(C_F/C)-1]$ vs. t, further prediction and design is then available.

Eq. (3.35) can also be expressed as :

$$\ln\left(\frac{C_F}{C}-1\right)=k'(t-t_1) \qquad (eq.\ 3.36)$$

where :

$k'=k_{Th}C_F$ and $t_1= q_F\, m/(QC_F)$. The general version of eq. (3.36) is represented as :

$$\ln\left(\frac{C_F}{C}-1\right)=b_o+b_1 t+b_2 t^2+\cdots=\sum_i b_i t^i. \qquad (eq.\ 3.37)$$

This equation is applied when $\ln[(C_F/C)-1]$ vs. t is not in linear form.

By fitting the experimental data, the corresponding parameters bi can be calculated.

Generally, it is adequately accurate to employ the former three terms. It is worth noting that q_F derived from the experiment is often conspicuously different from the

value acquired by equilibrium calculation, and the bed adsorptive capacity is often determined from the dynamic adsorption [52].

3.4.5. Bohart-Adams model and bed depth service time (BDST) model

Bohart and Adams (1920) came up with the Bohart-Adams (B-A) model when they proceeded with their work of analyzing the typical chlorine charcoal transmission curve [53].

They hypothesized that the uptake rate of chlorine is proportional to the concentration of the chlorine existing in the bulk fluid and the residual adsorptive capacity of charcoal, from which the following two equations are obtained:

$$\frac{\partial C}{\partial z} = -\frac{k_B q_r C}{u} \qquad \text{(eq. 3.38)}$$

$$\frac{\partial q_r}{\partial t} = -k_B q_r C \qquad \text{(eq. 3.39)}$$

where :

q_r = the residual adsorptive capacity, and

k_B =the kinetic constant of the Bohart-Adams model.

Additionally :

$$\begin{cases} t = 0 \rightarrow \dfrac{q_r}{q_m} = 1, \\ z = 0 \rightarrow \dfrac{C}{C_F} = 1. \end{cases}$$

Finally, the basic form of the B-A model was obtained:

$$\ln\left(\frac{C_F}{C} - 1\right) = \ln\left[\exp\left(k_B q_m \frac{H}{u}\right) - 1\right] - k_B C_F t. \qquad \text{(eq. 3.40)}$$

If exp ($k_B q_m H/u$) is much larger than 1, eq. (3.40) can be reduced and rearranged as:

$$t = \frac{q_m}{C_F u} H - \frac{1}{k_B C_F} \ln\left(\frac{C_F}{C} - 1\right).$$

(eq. 3.41)

Eq. (3.41) is the so-called bed depth service time model [54].

Note that the B-A model (or bed depth service time (BDST) model) involves several important variables of adsorption system such as C_F, u, q_m, and H, and approximate estimation of the effect of each parameter from both models is achievable. As two widely used models in practice, the B-A and BDST models succeeded in predicting several breakthrough curves and optimizing the parameters, although it is relatively rough.

Both the B-A and BDST models have seven parameters, among which CF and u can be determined before the dynamic adsorption experiment.

For the B-A model, the height of the fixed bed (i.e., the height of packing adsorbent), H, is a constant and can be directly measured. Subsequently, different C and corresponding t are obtained through the dynamic adsorption experiment, and then a plot of $\ln(C_F/C-1)$ vs. t should theoretically be a straight line.

After linear regression, q_m and k_B can be calculated from the tangent slope and intercept, respectively.

In terms of calculated q_m and k_B, prediction of adsorption performance at different process variables is available based on eq. (3.40).

As for the application of the BDST model, similar to the B-A model, after determining the demand concentration of the effluent solution, q_m and k_B can be worked out by a straight line of t vs. H.

Then, the adsorption efficiency, under various conditions can be predicted.

Actually, q_m and k_B are not constant when the variable(s) is changed, which may lead to unsatisfactory prediction. Especially, at 50% breakthrough, $C/C_F=0.5$ and $t=t_{1/2}$, and eq. (3.41) changes to:

$$t_{1/2} = \frac{q_m H}{C_F u}.$$

(eq. 3.42)

Hence, q_m can be calculated by plotting $t_{1/2}$ vs. H. By rearranging Eq. (3.41) into proper form or giving specific values to parameters, the BDST model is frequently employed as a powerful tool to find the optimal operation condition. More recently, Ko et al. (2000) came up with a method to optimize the BDST model, where the bed adsorptive capacity qm is substituted by a modified correlation [52]:

$$q_t = q_m\left[(1-\exp(-a_r\sqrt{t})\right].$$

(eq. 3.43)

Integrating into eq. (3.38) :

$$t = m'\left[(1-\exp(-a_r\sqrt{t})\right]z + b'.$$

(eq. 3.44)

a_r is the rate parameter, $m'=q_m/(C_F u)$, and $b'=-[1/(k_B C_F)]\ln[(C_F/C)-1]$.

This method provides a way to approximately evaluate the significance of both film diffusion and intrapellet diffusion. The intrapellet mass transfer rate is proportional to the square-root of the residence time when the sorption process is controlled by intrapellet diffusion [55]:

$$\frac{a_1}{a_2} = \sqrt{\frac{t_1'}{t_2'}} = \sqrt{\frac{u_2}{u_1}}.$$

(eq. 3.45)

According to the correlation proposed [56]:

$$Sh = \frac{1.09}{\varepsilon} Pe^{1/3}.$$

(eq. 3.46)

Namely :

$$\frac{a_1}{a_2} = \left(\frac{u_1}{u_2}\right)^{2/3} = \left(\frac{u_2}{u_1}\right)^{-2/3}.$$

(eq. 3. 47)

Combining Eq. (3.45) and Eq. (3.47), one can obtain :

$$\frac{a_1}{a_2}=\left[\left(\frac{u_2}{u_1}\right)^{1/2}\right]^{p_i}\left[\left(\frac{u_2}{u_1}\right)^{-2/3}\right]^{p_f}=\left(\frac{u_2}{u_1}\right)^{p'}$$

(eq. 3.48)

where :

p_i, p_f reflect the fractions of the overall uptake rate influenced by intrapellet diffusion and film diffusion, respectively. Thus,

$$\begin{cases}0.5p_i-\frac{2}{3}p_f=p',\\ p_i+p_f=1,\end{cases}$$

Where p′ is determined by fitting the experimental data so that pi and pf are acquired subsequently.

3.4.6. Yoon-Nelson model

The Yoon-Nelson model is extremely concise in form, supposing that the decrease in the probability of each adsorbate to be adsorbed is proportional to the probability of its adsorption and breakthrough on the adsorbent [57].

It can be represented by :

$$\ln\frac{C}{C_F-C}=K_{YN}t-t_{1/2}K_{YN}$$

(eq. 3.49)

where K_{YN} is the Yoon-Nelson rate constant.

By plotting $\ln[C/(C_F-C)]$ vs. t, K_{YN} and theoretical $t_{1/2}$ are reckoned.

The Yoon-Nelson model not only has a more simple form than other models, but also requires no detailed data concerning the characters of adsorbate and adsorbent, as well as the parameters of the fixed bed [58].

Also, as limited by its rough form, the Yoon-Nelson model is less valuable or convenient to obtain process variables and to predict adsorption under variety conditions.

3.4.7. Wang model

Wang et al. (2003) developed a mass transfer model to describe the breakthrough curve of solutions containing Co or Zn ions in the fixed bed on the basis of the following assumptions [59]:

(1) The adsorption process remains isothermal

(2) The mass transfer equation is written as

$$-\frac{dy}{dt} = k_w xy, \qquad \text{(eq. 3.50)}$$

Where :

k_w = the kinetic constant

y = the fraction of the adsorbed metal ions, and

x = the fraction of metal ions passing through the fixed bed, with x+y=1.

(3) The breakthrough curve is symmetrical and,

(4) There is negligible axial dispersion in the column.

Presuming y=yw at t=tw and integrating eq. (3.50), one can obtain :

$$\ln\left[x(1-x_a)/x_a(1-x)\right] = k_w(t_a - t). \qquad \text{(eq. 3.51)}$$

Let w=0.5, then $yw=y_{1/2}=x_{1/2}$, $t_w=t_{1/2}$. Combining the above parameters with eq. (3.51) :

$$t = t_{1/2} - \frac{1}{k_w}\ln\left(\frac{1}{1-x}\right), \qquad \text{(eq. 3.52)}$$

where x can be expressed as :

$$x = C/C_F. \qquad \text{(eq. 3.53)}$$

Substituting eq. (3.53) into eq. (3.52), t should be in direct proportion to ln[(C_F/C)−1]. A plot of ln[(C_F/C) −1] vs. t produces the slope and intercept value as 1/kw and t1/2, respectively.

Then the entire breakthrough curve can be obtained based on Eq. (3.52). Meanwhile, similar to the Yoon-Nelson model, it cannot provide sufficient information of an adsorption system.

3.4.8. Wolborska model

Wolborska and Pustelnik (1996) analyzed the adsorption of p-nitrophenol on activated carbon and found that the initial segment of the breakthrough curve is controlled by film diffusion with constant kinetic coefficient, and the concentration profile of the initial stage moves axially in the column at a constant velocity[60].

Moreover, the width of concentration profile in the column and the final breakthrough curve were nearly constant. Based on above observations, they developed a model to describe the breakthrough at low concentration region, which was written as:

$$\ln\frac{C}{C_F}=\frac{\beta_L C_F \varepsilon}{\rho q_F}t-\frac{\beta_L H}{u} \qquad \text{(eq. 3.54)}$$

where β_L is the film diffusivity, which can be determined from the initial linear section of the breakthrough curve in the semi-logarithmic system through experiment or correlations.

3.4.9. Modified dose-response model

This model was initially developed for pharmacology studies and recently used to describe adsorption of metals in some cases, e.g. as in [61]. The modified dose-response model can be written as:

$$\frac{C}{C_F}=1-\frac{1}{1+\left(\frac{C_F Q t}{q_F m}\right)^{a'}}. \qquad \text{(eq. 3.55)}$$

After rearrangement, it could be written as:

$$\ln\frac{C}{C_F - C} = a'\ln(C_F Qt) - a'\ln(q_F m)$$

(eq. 3.56)

where α′ is the model parameter. Similar to other models, α′ and q_F could be determined by plotting $\ln[C/(C_F - C)]$ vs. $\ln(C_F Q_t)$.

CHAPTER 4 : BIOMASS AS ADSORBENT - BIOSORPTION TECHNOLOGY

4.1. Introduction-General Remarks

The search for a low cost and easily available adsorbent has led to the investigation of materials of agricultural and biological origin, along with industrial by-products, as adsorbents.

Microorganisms such as bacteria, fungi, yeast and algae can remove some pollutants from aqueous solutions and this biological phenomenon is called **biosorption** [51].

This term is used to indicate a number of metabolism-independent processes (physical and chemical adsorption, ion exchange, complexation, chelation and microprecipitation) taking place essentially in the cell wall.

The main attraction of biosorption are cost effectiveness and good removal performance; raw materials which are either abundant (sea weeds) or wastes from other industrial operations (fermentation wastes, activated sludge process wastes) can be used as biosorbents presenting performances often comparable with those of ion exchange resins [51,62].

The mechanism of binding by inactivated biomass may depend on the chemical nature of pollutant (species, size, ionic charge), type of biomass, its preparation and its specific surface properties and environmental conditions (pH, temperature, ionic strength, existence of competing organic or inorganic ligands in solution).

As hydrophobic organic pollutants show a high tendency to accumulate onto microbial cells or sludge, the microbial biomass could be used as an adsorbent of biological origin for the removal of very lowconcentration hazardous organics from the wastewater. For all these reasons biosorption can be considered a promising technology for phenol removal from industrial waste streams and polluted natural waters [62].

Both living and dead biomass can be used to remove hazardous organics, but maintaining a viable biomass during adsorption is difficult, because it requires a continuous supply of nutrients and avoidance of organic toxicity to the microorganisms.

The use of dead microbial cells in biosorption is more advantageous for water treatment in that dead or organisms are not affected by toxic wastes, they do not require a continuous supply of nutrients and they can be regenerated
and reused for many cycles.

However, the use of dead biomass in powdered form has some problems, such as difficulty in the separation of biomass after biosorption, mass loss after regeneration and low strength and small particle size, which make it difficult to use in column applications[62,63].

To solve these problems, dead biomass can be immobilized in a biopolymeric or polymeric matrix used as a supporting material. Immobilization may improve biomass performance, biosorption capacity, increase mechanical strength and facilitate separation of biomass from pollutant-bearing solution. Immobilization also allows higher biomass concentration, resistance to chemical environments and column operations and immobilized systems may be well suited for non-destructive recovery. Indeed, the use of immobilized biomass has a number of major disadvantages. In addition to increasing the cost of biomass pre-treatment, immobilization adversely affects the mass transfer kinetics of phenol uptake.

When biomass is immobilized the number of binding sites easily accessible to pollutant in solution is greatly reduced since the majority of sites will lie within the bead.

So a good support material used for immobilization should be rigid, chemically inert and cheap, should bind cells firmly, should have high loading capacity and should have a loose structure for overcoming diffusion limitations [62,63].

For continuous operation with immobilized biomass, the most convenient configuration is that of a packed column, much like that used for ion exchange. A packed bed column is an effective process for cyclic sorption/desorption, as it
makes the best use of the concentration difference known to be a driving force for adsorption and allows more efficient utilization of the sorbent capacity and results in a better quality of the effluent [63].

Continuous packed bed sorption has also a number of process engineering advantages including high yield operations and relatively easy scaling up from a laboratory scale procedure. The stages in the separation protocol can also be automated and high degrees of purification can often be achieved in a single step process.

A large volume of wastewater can be continuously treated using a defined quantity of sorbent in the column. Reuse of microorganism is also possible. After pollutant loading the pollutant may be concentrated in a small volume of solid material or desorbed into a small volume of effluent for recovery, disposal or containment [62,63,64].

Activated sludge is a well known biomass used for the purification of some industrial effluents and domestic wastes. Part of the microorganisms over grown in such wastewater systems can be separated and utilized for removal of phenol as an abundant and cheaper biosorbent.

Activated sludge from wastewater systems contains both bacteria and protozoa. The cell wall of bacteria essentially consists of various organic compounds such as carboxyl, acidic polysaccharides, lipids, amino acids and other components.

The protozoa are unicellular, motile, relatively large eucaryotic cells that lack cell walls. They can absorb components through their outer membranes that contain proteins and lipids [63,6].

Mowital®B30H resin (a polyvinyl butyral based polymer) is a well known polymer used extensively in painting and coating industries. While it is abundant, extremely cheap than other immobilizing agents, non toxic and chemically inert, more suitable for preparation of porous beads, the solid and rigid support, showing little change in volume under any conditions, with dimensional stability under pressure, produced in the desired size and thus highly competitive with ion exchange resins and activated carbon so it can be used for immobilization of microorganisms for biosorption [65].

Activated sludge has been immobilized in Mowital®B30H resin in order to produce a biosorbent material with proper characteristics for use in typical chemical engineering operations such as fixed beds.

It has been used to demonstrate the potential for removal of phenol from waste streams in a continuous packed bed column as a function of flow rate and inlet phenol concentration. The column phenol sorption equilibrium has been described by the use of Langmuir and Freundlich models.

Wastewater discharge from electroplating, electronics, and metal cleaning industries often contains high concentrations of nickel(II) ions and causes serious water pollution. The presence of nickel(II) ions above critical levels may cause various types of acute and chronic disorder in human health, such as severe damage

of lungs and kidney, gastrointestinal distress (e.g. nausea, vomiting, and diarrhea), pulmonary fibrosis and renal edema, and skin dermatitis [66].

The conventional technologies of high concentration heavy metal ions removal from wastewater are the precipitation processes, membrane filtration, ion exchange, evaporation, electro- chemical processes, etc. The main disadvantages of mentioned technologies are the high cost of implantation and operations, for concentrations below 100 mg/L [67].

Hence, the new technologies with acceptable costs are necessary for reduction of the heavy metals concentration in industrial effluents. One of the promising alternatives is application of biosorption process that uses the living or dead organisms as an adsorbent such as fungus, bacteria, and seaweed [68,69].

The accumulated knowledge about biosorption mechanism is the base of the invention of new technologies to remove heavy metals from diluted solutions (1–100 mg/L)[70].

An additional advantage of the biosorption process is considered to be the low costs of used bioadsorbent, which can be obtained as a residue from bio-industries (fermentation bio-products) or biomass found in nature (marine algae) [71].

The biosorption mechanism, using as biosorbent marine algae, can involve the combination of one or more phenomena such as ion exchange, complexation, physical and/or chemical adsorption, coordination, and inorganic microprecipitation.

Among these unit processes, the ion exchange is considered to be the key one involved in the biosorption procedure [72].

Most separation and purification processes that use sorption technology involve continuous flow operations. In this operating mode, the saturated solid sorbent zone gradually extends throughout the column where the sorbate is adsorbed.

The adsorption experimental data show a typical S-shaped curve where the slope is a result of three factors: the equilibrium sorption isotherm relationship, mass transfer effects throughout the sorbent in the column, and the influence of axial mixing, which determines deviation from the ideal plug-flow behavior [73].

Fixed bed columns systems with continuous flow allow the regenerating cycles operation. Using an appropriate effluent solution, the sorbent can be regenerate. The regeneration process liberates small volumes of concentrated metal solutions, which are more appropriate for conventional recovery processes [74].

To represent a dynamic heavy metals ions removal in fixed bed columns, a mathematical analysis of the system was performed and S-shaped experimental curves were evaluated.

A typical breakthrough curve can be represented as a ratio of the effluent (C) and inlet concentration (C_0) versus time. The efficiency of the adsorption process can be estimated by sharpness of the breakthrough curve.

The correct design of a fixed bed column used for biosorption is not easy task and to reduce the costs of implementation of such equipment mathematical models have to be applied as the most robust and powerful tool.

The model validation is performed on the bases of experimental data collected from laboratory scale, and statistical criterion is used during the non-linear parameter identification procedure. The developed models then may be applied for designing and process optimization in pilot plant and industrial scale [75].

The residence time is a key parameter in the design procedure of adsorption in fixed bed column [76].

When operating with low flow rates, the process is controlled by the external mass transfer (fluid around the particles surface) limitation.

To avoid such a control, it is suggested for the process to operate in the range of higher flow rates. High flow rates may be applied in a process that is controlled by the internal mass transfer velocity (diffusion inside the particles).

However, this will result in low residence times for adsorption and therefore, a decreasing of flow rates is suggested. It is obvious that the two effects are antagonistic and the optimal flow rate has to be searched in the intermediate region of flow rates Hence, the mass transfer coefficients have to be determined correctly to guarantee an optimal column design[77].

The mathematical models used to describe the adsorption process can be divided in three categories: models of equilibrium stage, theory of the interference, and models of rate equation.

The models of rate equation are more realistic compared to the others. These models are based on the species mass balances of interest in both, the fluid and the stationary phase (sorbent particles).

They generally consider the effect of mass transfer in the liquid film, intraparticle diffusion, and equilibrium isotherms.

Due to the complexity and non-linearity of these models, general analytical solutions are usually impossible to be achieved [78].

There are several mathematical models in the literature, which have been used to represent the dynamics of the fixed bed column.

Models with analytical solutions [79,80] are often used for fitting the breakthrough curve. However, these models need to be revised for mono-component systems; moreover, some assumptions are necessary to be made to achieve an analytical solution.

Otero et al. [81] have investigated the phenol composite removal in fixed bed column. The applied model for the fixed bed adsorption has considered mass balance in the fluid phase, the adsorption equilibrium isotherm at the liquid/solid interface, and a linear driving force rate equation describing the diffusional mass transfer inside adsorbent particles.

In this model, the ion diffusion limitation in the external film and the ion diffusion limitation in the adsorbent were connected to a global mass transfer coefficient. According to this author, the rate of adsorption is proportional to the driving force, which is the difference between the concentration in the adsorbed phase in equilibrium with the fluid phase bulk concentration and the average adsorbed concentration in the particle.

Recently, several researchers [73,82–85] have used the linear driving force model to represent the rate equation.

The most of the models consider only one limiting stage during the adsorption process. This assumption facilitates the resolution of the model, reducing the number of equations, which have to be solved.

Mathematical models that incorporate mass transfer limitations can be used for prediction of the characteristic breakthrough curves. However, for accurate prediction, such models require reliable experimental data with respect to the feeding conditions and to the parameters associated with the mass transfer processes: diffusion limitation in the liquid film around the adsorbent particles and diffusion limitation of solute inside the adsorbent.

A more sophisticated model considering double limitation effects to represent the adsorption dynamics in fixed bed was developed by Hsieh et al. [86].

A necessary, but not sufficient requirement for an adequate description of the sorption dynamics in fixed bed columns is for the mathematical formulas (adsorption isotherm,

ion exchange isotherm, mass action law) to appropriately represent the equilibrium data among the phases in the column [75,87].

The ion exchange which has been identified as a main mechanism in the biosorption process and the equilibrium data are usually represented by adsorption isotherms such as: Langmuir, Freundlich, Sips, Redlich–Peterson.

In the ion exchange isotherms, the effect of the released ion from the adsorbent is considered in the equations. It should be noted that, when the affinity of these ions is small compared with the metal uptake, this effect could be neglected. Usually, the Langmuir isotherm is used for the equilibrium description between the solid and liquid phases in an adsorption process.

The constants in the Langmuir isotherm have physical meaning, where parameter (K) represents the ratio of adsorption and desorption rates. High values of this parameter indicate a strong affinity of the ion to the material sites. The parameter q_{max} represents the total number of available sites in the material adsorbent.

Analyzing the results achieved in the area of heavy metal ion removal by biosorption, one can see that a challenging problem is the modeling of the fixed bed column containing biosorbent[87].

4.2. Case Study 1: Copper biosorption on immobilized seaweed biomass

4.2.1. Introduction

One form of biomass that has shown impressive metal binding properties is marine macroalgae, commonly referred to as seaweeds [88].

Seaweeds are a widely available source of low-cost biomass as over two million tonnes are either harvested from the oceans or cultured annually for food or phycocolloid production. [89].

Various species of seaweeds have been tested in the laboratory for removal of a range of toxic metal ions. [90].

For industrial-scale operation biosorption can be easily implemented using the well-established activated carbon fixed-bed system since design procedures as well as process equipment for this type of operation are readily available (Cooney, 1999).

It is therefore desirable to develop biosorption processes for metal removal based on the fixed-bed configuration.

Although seaweed biomass in its native form has been used in fixed-bed studies, e.g. (Cossich et al., 2004), the biomass in general has a tendency to disintegrate and swell, causing operational problems such as clogging and pressure drop fluctuations. To be of practical use, seaweed biomass can be immobilized onto porous solids to increase its stability and mechanical strength.[91].

Many natural and synthetic polymers have been used for biomass immobilization. In the case of seaweed biomass immobilization, polyvinyl alcohol have been successfully used.

Polyvinyl alcohol (PVA) is a type of synthetic polymer that is readily available, cheap, and possesses excellent attrition resistance properties.

The broad objective of this study is to present a series of laboratory investigations carried out to evaluate the pertinent properties of PVA-immobilized seaweed biomass for its use in fixed-bed systems for copper removal.

Theoretical analysis using a simplistic fixed-bed model is also included in the study.

4.2.2. Materials

Samples of the brown seaweed *Sargassum baccularia* were collected from the west coast of Peninsular Malaysia.

The biomass was washed thoroughly to remove adhering sand and dried to a constant weight. It was then ground and sieved to a size range of 250–500 μm.

Polyvinyl alcohol (MW = 72000), disodium salt of ethylenediamine-tetraacetic acid (EDTA), copper nitrate salt, boric acid, and sodium phosphate were obtained from Fluka, Switzerland.

4.2.3. Biomass immobilization

An immobilization method published in the literature (Chen and Lin, 1994) was adopted in this work to immobilize seaweed particles onto PVA beads. Seaweed

particles were mixed with an aqueous PVA solution (15%, w/v) to produce a mixture with a solid-to-liquid ratio of approximately 150 g/L [92].

The resulting mixture was transferred to a syringe and released into a gently stirred saturated boric acid solution to form spherical beads. The beads were then transferred to a sodium phosphate solution for hardening, followed by washing with distilled water to remove residual chemicals.

4.2.4. Column experiments

PVA-immobilized biomass beads were packed in a glass column with a diameter of 1.6 cm to a height of 10 cm.

The temperature of the water-jacketed column was maintained at 25°C. Distilled water adjusted to pH 5 was pumped through the column using a liquid chromatography pump (Perkin Elmer, USA) to condition the beads.

Three column tests were performed to determine breakthrough curves at

Different flow rates (1 or 1.5 ml/min) and feed concentrations (20 or 40 mg/L).

A feed solution of known copper concentration adjusted to pH 5 was pumped through the column at a known flow rate.

Samples were collected at the column outlet at fixed time intervals and analyzed for copper concentration using an inductively coupled plasma atomic emission spectrophotometer (ICP-AES) (ICP 2000, Baird, USA).

In the experiments consisting of multiple biosorption/ desorption cycles, the biosorbent column was first loaded with copper.

Upon saturation, the feed flow was replaced with a distilled water flow to flush out any unbound copper from the column.

Aqueous solution containing 2 mmol/L EDTA was then pumped through the column to elute the bound copper from the beads. Samples were collected at the column outlet at fixed time intervals and analyzed for copper by the ICP-AES.

At the end of the elution step, distilled water adjusted to pH 5 was pumped into the column to recondition the beads and to displace any remaining EDTA solution that might interfere with the next cycle of copper loading.

The biosorbent column, now free of copper and EDTA, was ready for reuse.

The above experimental procedure constituted one cycle of copper loading and elution. Three consecutive cycles were conducted to assess the performance of PVA-immobilized biomass beads under continuous flow conditions.

4.2.5. Results and discussion

Fig.4.1a shows the experimental breakthrough curves (points) for a feed containing 20 mg/L copper obtained at two different flow rates, while Fig.4.1b displays those for two different feed concentrations measured at a flow rate of 1 ml/min.

Breakthrough curves calculated from a theoretical model are also included in Fig4.1 (lines) and these are discussed later.

Fig.4.1a shows that when the flow rate increased from 1 to 1.5 ml/min the time required for complete column saturation decreased from 900 min to about 600 min.

The breakthrough curve obtained at the higher flow rate shows a much shorter clear period (i.e., undetectable effluent copper concentration) before the breakthrough point (the point that copper was first detected in column euent) and a much sharper shape.

Increasing the feed concentration produced a similar trend, as shown in Fig.4.1b; the breakthrough curve shifted towards the origin with increasing feed concentration.

The slope of the breakthrough curve for the 20 mg/L feed is noticeably less sharp than that of the breakthrough curve for the 40 mg/L feed.

Mathematical models are useful for understanding fixed-bed column dynamics and for design and optimization studies since they help reduce time-consuming and repetitive experiments.

Various fixed-bed models of varying complexity have been used to study the dynamics of immobilized biosorbent systems (Cossich et al., 2004) understanding of the dynamics of fixed-bed columns, their practical utility is rather limited owing to the complicated solution methods [91].

On the other hand, simplified models are useful when it is desired to develop a practical tool that can capture quantitatively the effects of main system variables on the column dynamics.

In this work, the ability of a relatively simple fixed-bed model, known as the Bohart-Adams equation [79] to describe the breakthrough behavior of PVA-immobilized biomass beads was examined. The development of the Bohart- Adams model follows.

We consider an isothermal column packed with a biosorbent through which a fluid containing a metal ion flows with constant linear velocity.

The differential mass balance for the column is given by[79]:

$$v\frac{\partial C}{\partial z}+\frac{\partial C}{\partial t}+\left(\frac{1-\varepsilon}{\varepsilon}\right)\frac{\partial q}{\partial t}=D_L\frac{\partial^2 C}{\partial z^2} \qquad \text{(eq. 4.1)}$$

Where :

C = the fluid phase metal concentration,

q = the metal concentration in the biosorbent averaged over the biosorbent volume

ν= the interstitial velocity

D_L = the axial dispersion coefficient

ε = the column void fraction

z = the axial coordinate with origin at the column inlet, and

t = represents time.

The initial and boundary conditions for the column initially free of metal and subjected to a step change in metal concentration at the column inlet at time zero are given by:

$$t=0,\ C=q=0$$

$$z=0,\ \frac{D_L}{v}\frac{\partial C}{\partial z}=C-C_0$$

$$z=L,\ \frac{\partial C}{\partial z}=0$$

Where :

C_0 = the metal concentration of the feed solution

L= the column length.

The term $\partial q/\partial t$ in eq.(4.1) represents the local rate of adsorption between the fluid and biosorbent phases.

Various dynamic models have been derived which differ mainly in the choice of kinetic rate expression.

The Bohart-Adams model assumes that adsorption can be described by a quasi-chemical kinetic rate expression:

$$\frac{\partial q}{\partial t} = bC\,(q_s - q)$$

(eq. 4.2)

Where :

q_s = the saturation capacity of the biosorbent

b = a rate constant.

Neglecting axial dispersion, the analytical solution to eqs.(4.1) and (4.2), first obtained by Bohart and Adams (1920),[79] is given by:

$$\frac{C}{C_0} = \frac{\exp\left(bC_0\left(t - \frac{L}{v}\right)\right)}{\exp\left(bC_0\left(t - \frac{L}{v}\right)\right) + \exp\left(\frac{bq_sL}{v}\left(\frac{1-\varepsilon}{\varepsilon}\right)\right) - 1}$$

(eq. 4.3)

A useful approximation to Eq.(4.3) is to assume t>> L/v and to disregard the "1" term in the denominator [93]. These two simplifications allow us to express eq.(4.3) as:

$$\frac{C}{C_0} = \frac{1}{1 + \exp\left(b\left(a\frac{L}{u} - C_0t\right)\right)}$$

(eq. 4.4)

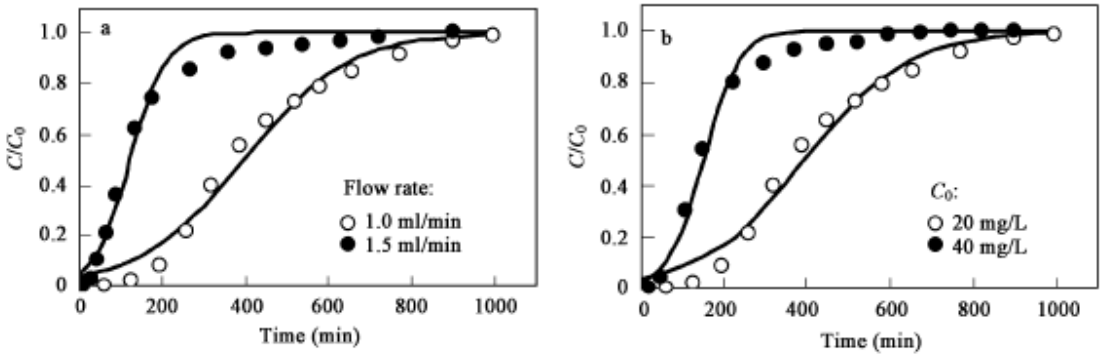

Figure. 4.1 .Effect of flow rate on breakthrough curves at feed concentration of 20 mg/L (a) and effect of feed concentration (C_0) on breakthrough curves at flow rate of 1 ml/min (b). Points are experimental, curves are best-fitting model simulations obtained from eq.(4.4).[93]

where,

u is the superficial velocity ($u = \varepsilon v$) and α is the saturation capacity of the biosorbent per unit volume of the packed bed ($\alpha = q_s(1 - \varepsilon)$). Upon rearrangement, eq.(4.4) becomes:

$$t = a\frac{L}{uC_0} - \frac{1}{b}\frac{\ln\left(\frac{C_0}{C} - 1\right)}{C_0} \qquad \text{(eq. 4.5)}$$

According to eq.(4.5), plotting experimental data in terms of t versus $\ln(C_0/C–1)/C_0$ should yield straight lines and the two parameters a and b can be estimated from the corresponding intercepts and slopes, respectively.

Note that the Bohart-Adams model is sometimes inadvertently referred to as the Thomas model in the biosorption literature.

Nonetheless, the Bohart-Adams model is closely related to the Thomas model and can be regarded as a limiting form of the latter [94].

Fig.4.2 displays the breakthrough data of Figs.4.1a and 4.1b plotted in terms of eq.(4.5).

In all cases, a linear relationship between *t* and $\ln(C_0/C–1)/C_0$ is not found, indicating that the experimental results do not conform to the linearized Bohart-Adams model. The implication is that *a* and *b* cannot be estimated from these nonlinear curves.

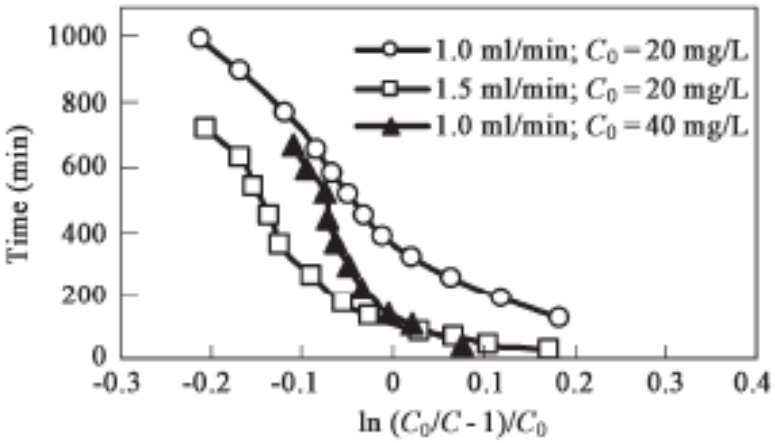

Fig.4. 2 Experimental breakthrough data plotted according to Eq.(4.5)

An alternative method of estimating a and b is to fit eq.(4.4) directly to the breakthrough data of Figs.4.1a and 4.1b by a nonlinear least-squares fit. The values of a and b obtained using this approach are tabulated in Table4.1.

Calculated curves using these values for a and b are shown as lines in Figs.4.1a and 4.1b, in comparison with the experimental data. Overall, the agreement between the experimental curves and calculated ones is approximate.

In particular, the model overestimated the sharpness of the leading and trailing edges of the experimental breakthrough curves.

Table 4.1 Best-fit values of Bohart-Adams parameters obtained by fitting eq.(4.4) to experimental breakthrough curves

Flow rate (ml/min)	C_0 (mg/L)	Bohart-Adams parameters	
		a (mg/L)	b (L/(mg·min)
1.0	20	393.64	0.4×10^{-3}
1.5	20	184.90	1.2×10^{-3}
1.0	40	302.48	0.5×10^{-3}

The discrepancies between the measured and calculate breakthrough curves can be ascribed to the approximations inherent in using the simplistic Bohart-Adams model, which is capable of generating symmetrical, sigmoidal breakthrough curves.

The nonlinear plots in Fig.4.2 indicate that the experimental breakthrough curves reported here are asymmetrical.

The broadness of the trailing edge of the breakthrough curves could perhaps result from slow intraparticle diffusion within the pores of the biosorbent beads. Copper must first diffuse into the porous beads before interacting with the functional groups of *Sargassum* biomass.

The "tailing" of a breakthrough curve (i.e., a slow approach of C/C_0 towards 1) is commonly observed in liquid phase adsorption where intraparticle diffusion is the dominant mass transfer process.[94].

The Bohart-Adams model does not explicitly account for the phenomenon of intraparticle diffusion as it uses a quasi-chemical kinetic rate expression to describe mass transfer.

4.3. Case Study 2 : Removal of lead (II) ions from effluents using immobilized *Pinus sylvestris* sawdust: Adsorption on a fixed-bed column

4.3.1. Introduction

The removal of toxic heavy metal contaminants from aqueous waste streams is currently one of the most important environmental issues being researched.

Although this issue has been studied for many years, effective treatment options are still limited.

Chemical precipitation, ion exchange, reverse osmosis and solvent extraction are the methods most commonly used for removing heavy metals ions from dilute aqueous streams [95].

Studies carried out to look for new and innovative treatment technologies have focused attention on the metal binding qualities of various types of biomass [96,97].

It was shown that some microorganisms and biomass are able to adsorb toxic and heavy metals from dilute aqueous so lutions.

The factors affecting the metal binding qualities of these biomaterials or their affinity for a metal dissolved in aqueous media include:

(i) the chemical nature of the metal ions (e.g. size, valence, electron orbital structure, stability of the chemical forms in nature) and that of the biomass (e.g. charge density and structure of the polymer chain, functional groups),

(ii) medium conditions (e.g., pH, temperature, ionic strength, presence of competing organic or inorganic metal chelators). Biosorptive processes are

generally rapid and theoretically suitable for extracting metal ions from large volumes of water [98].

Results obtained in previous studies carried out on a batch reactor showed that the removal of lead and cadmium through their binding onto *Pinus sylvestris* sawdust is possible.

The latter biomaterial contains various organic compounds such as lignin (with polyphenolic groups), cellulose (with numerous hydroxyl functions) and hemicelluloses (with carboxylic and hydroxyl groups).

These functional groups may be useful for binding ions of heavy metals [99].

Although various types of reactors, e.g. batch, continuously stirred tank reactors and fluidized-bed columns can be used, adsorption on packed bed columns presents numerous advantages.

It is simple to operate, gives high yields and can be easily scaled up from a laboratory process.

The purpose of this study was to investigate the influences of bed depth, linear flow rate and concentrations of feed metal ions on the performance of lead (II) adsorption onto *P. sylvestris* sawdust immobilized in a packed-bed column.

This work was firstly carried out on a mini-column and the results were then checked on a pilot scale unit.

4.3.2. Methods

In this work, studies were starting from the mass balance of the packed-bed reactor. The variation of this balance during the reaction can be illustrated by Fig. 4.3, where u is the linear flow rate, which is the average rate of the liquid flow when the column is empty.

The equation of mass balance material is: input flow= output flow+ flow inside pores volume + matter adsorbed onto sawdust.

For this system, the balance can be expressed according to the following equation :

$$Q_v C_0 = Q_v C + V_p \frac{dC}{dt} + m \frac{dq}{dt} \qquad \text{(eq. 4.6)}$$

where :

Q_v = the volumetric flow of the solution in the column (l min^{-1}),

Q_0 and C, respectively,= the inlet and outlet solute concentrations (mg. l^{-1}),

QvC_0 =the inlet flow of solute in the column (mg. min^{-1}),

QvC =the outlet flowof solute leaving the column (mg. min^{-1}),

Vp = the porous volume (l) (Vp = $\frac{\tilde{1}}{\tilde{1}-\varepsilon} V_a$

Where Va is the bulk volume and ε the porosity), $V_p \frac{\tilde{d}C}{dt}$ the flow rate through the bed depth column (mg .min^{-1}) and $m \frac{dq}{dt}$ the amount of solute adsorbed onto sawdust (mg. min^{-1})

Where :

m = the mass of sawdust and

$\frac{dq}{dt}$ = the adsorption rate.

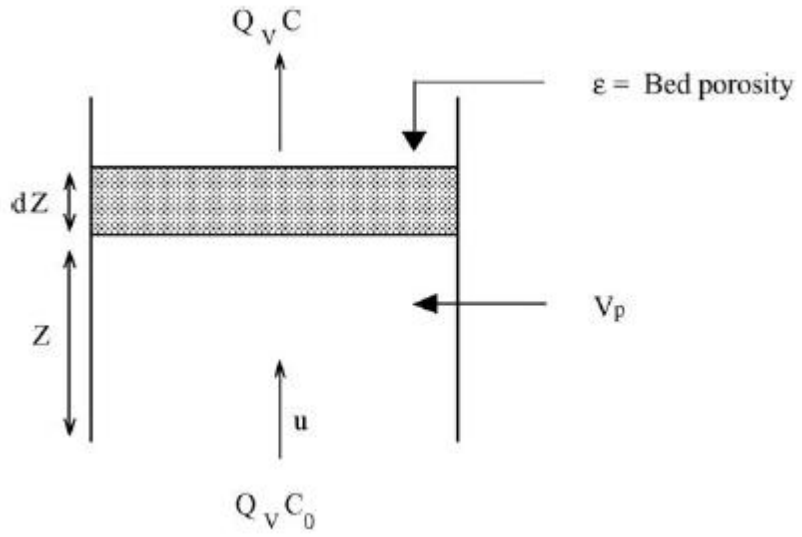

Figure 4.3. Scheme of bed depth [100]

According to relation (1), the determining factors of thebalance for a given bed depth of the column are the linear flow rate (u = Qv/S_c where Sc is the column section, m^2), the initial solute concentration, the adsorption potential and the porous volume even if previous studies showed that the latter parameter may be neglected.

Therefore, in order to optimize the adsorption process in a packed-bed column, it is necessary to examine these parameters and to estimate their influence.

Several types of reactors were used for the adsorption processes in a continuous system: adsorption within a fixed-bed column and adsorption with a fluidized-bed column.

It is necessary to note that the fixed-bed regime presents numerous advantages in a pilot plant notably its precision and bed performance, whereas in the industrial scale-up the fluidized bed is more advantageous particularly as it seals out the biomass and also reduces the risks of saturation in the columns.

4.3.2.1. Design of the adsorption column based on bed depth service time (BDST)

Adsorption within a packed-bed column is a process in which a continuous mass transfer occurs between two phases (the mobile phase containing the solute and the solid phase of the packed bed). The solute concentration in both phases is a function of the contact time and the depth of the adsorption zone.

A mathematical model based on mass balance is often used to explain the adsorption phenomena and to find out the characteristic variables of the process. Several models can be used.

This work aims to study the effect of various experimental conditions on the bed depth service time (BDST) model and then to compare the obtained results with those of previous studies [100].

The BDST model describes a relation between the service time of the column and the packed-bed column. The original work on the BDST model was carried out by Bohart and Adams [79] on the adsorption, in dynamic system, of the chlorine onto activated charcoal and those of Thomas [80] on the adsorption of the ions by zeolites.

Working on the model, the authors supposed that intraparticular diffusion and external mass resistance are negligible and the adsorption kinetics is controlled by the surface chemical reaction between the solute in the solution and the adsorbent not yet used [9]. The authors demonstrated that the system agrees with eq. (2) [99,100]:

$$\ln\left[\frac{C_0}{C_b} - 1\right] = \ln\left(e^{(k_{ads}N_0/u)z} - 1\right) - k_{ads}C_0 t_b \qquad \text{(eq.4.7)}$$

In this relation $e^{(k_{ads}N_0/u)z} \gg 1$, thus $\ln(e^{(k_{ads}N_0/u)z} - 1) \cong \frac{k_{ads}N_0}{u}Z$, that is the reason why the following linear relation between the column bed depth (Z) and the service time (t_b) holds true:

$$t_b = \frac{N_0}{C_0 u}Z - \frac{1}{k_{ads}C_0}\ln\left(\frac{C_0}{C_b} - 1\right) \qquad \text{(eq. 4.8)}$$

Where :

t_b = the service time at breakthrough point (min),

N_0 = the dynamic bed capacity (mg l^{-1}),

Z = the packed-bed column depth (m),

u = the linear flow rate (m. min^{-1}) defined as the ratio of the volumetric flow rate Qv(m^3. min^{-1}) to the cross-sectional area of the bed S_c (m^2), C_0 and C_b are, respectively, the inlet and the breakthrough metal ions concentration (mg l^{-1}) and k_{ads} the adsorption rate constant (l. mg^{-1} min^{-1}).

Eq. (4.8), known under the name of bed depth service time (BDST) can be determined for a given adsorbent depth and is a straight line:

$$t_b = m_x Z - C_x \qquad \text{(eq. 4.9)}$$

Where mx = (min.m^{-1}) is the slope of the BDST line and represents the time required for the adsorption zone to travel a unit length through the adsorbent [100]. It is used to predict the performance of the bed. Cx is the abscissa intercept in the BDST plot.

The dynamic bed capacity (N_0) and the adsorption rate constant (k_{ads}) can be evaluated from the slope and intercept of the plot of t_b versus Z.

The bed depth (Z_0), which represents the theoretical depth of adsorbent able to prevent the adsorbent concentration from exceeding Cb, is obtained when tb = 0, according to the following equation:

$$Z_0 = \frac{u}{k_{ads}N_0}\ln\left(\frac{C_0}{C_b} - 1\right) \qquad \text{(eq. 4.10)}$$

By varying the column bed depth (Z), the plot of Eq. (4.8) allows to calculate the value of N_0 and thus to estimate the value of Z_0.

If there is a change in the initial solute concentration C_0 to a new value C_0' the new values of m'$_0$ and C'$_x$ can be, respectively, obtained from the slope and the intercept according to the relations proposed by Hutchins [100]:

$$m'_x = m_x \left(\frac{C_0}{C'_0} \right) \qquad \text{(eq. 4.11)}$$

$$C'_x = C_x \left(\frac{C_0}{C'_0} \right) \frac{\mathrm{Ln}\left(\frac{C'_0}{C_b} - 1 \right)}{\mathrm{Ln}\left(\frac{C_0}{C_b} - 1 \right)} \qquad \text{(eq. 4.12)}$$

Where :

C_0 = the inlet solute concentration (mg l^{-1}) and

C'$_0$ = the new inlet value (mg l^{-1}).

When the linear flowrate is changed

from u to u', the new value of the slope (m'$_x$) is obtained by Eq. (4.13) [100].

However the intercept remains unchanged because it depends on the inlet solute concentration C_0:

$$m'_x = m_x \left(\frac{u}{u'} \right) \qquad \text{(eq. 4.13)}$$

4.3.2.2. Mass transfer zone

The mass transfer zone (MTZ) is the active surface of the sawdust bed in which adsorption occurs (Fig. 4.4).

The fluid flowing into the column gets through a virgin bed. The top of the adsorbent in contact with the fluid quickly adsorbs the pollutant during the first contact. Thus the fluid leaving the column is practically free of metallic ions (points P1, P2 and P3 in Fig. 4.4).

As the volume of polluted fluid getting through the bed column increases, an adsorption zone of mass transfer (MTZ) gets defined. In this MTZ, adsorption is

complete and the concentration of pollutant in the bed column varies from 100% of C_0 (corresponding to total saturation) to approximately 0% of C_0 (corresponding to the virgin adsorbent).

This adsorption zone then moves downwards through the bed column in relation to time until the breakthrough occurs.

When this zone reaches the bottom of the bed the pollutant dissolved in the solution cannot yet be adsorbed any longer. This moment is called "breakpoint". The plot obtained after this point gives the concentration history and is called breakthrough profile or breakthrough curve.

From a practical point of view, this point allows to determine the solute concentration in the effluent and the volume treated (Vb).

For most adsorbent–pollutant systems, the breakthrough curve is obtained after an effluent concentration of 50% has been reached. To facilitate the calculations of the bed adsorption capacity, the breakthrough curve is often fixed at 50% (P4, Fig. 4.4), sometimes at 10% (P3, Fig. 4.4) of the inlet concentration according to the target quality of the final effluent [12].

When the mass transfer zone leaves the bed column (P5, Fig. 4.4), the bed is completely saturated, adsorption in the bed does not occur and the effluent which leaves the column has the same concentration as the one that enters. The quantity of adsorbed pollutant at breakpoint (q_b in mg .g^{-1}) can be obtained from the following relation [13]:

$$q_b = \frac{Q_v t_{10\%} C_0}{m_c} \qquad \text{(eq. 4.14)}$$

Where :

$t_{10\%}$ = the service time (min) obtained when the outlet concentration is 10% of the inlet one,

C_0 = the inlet metal ions concentration (mg l^{-1}),

Q_v= the effluent volumetric flow rate (l min^{-1}) and

m_c = the amount of sawdust (g).

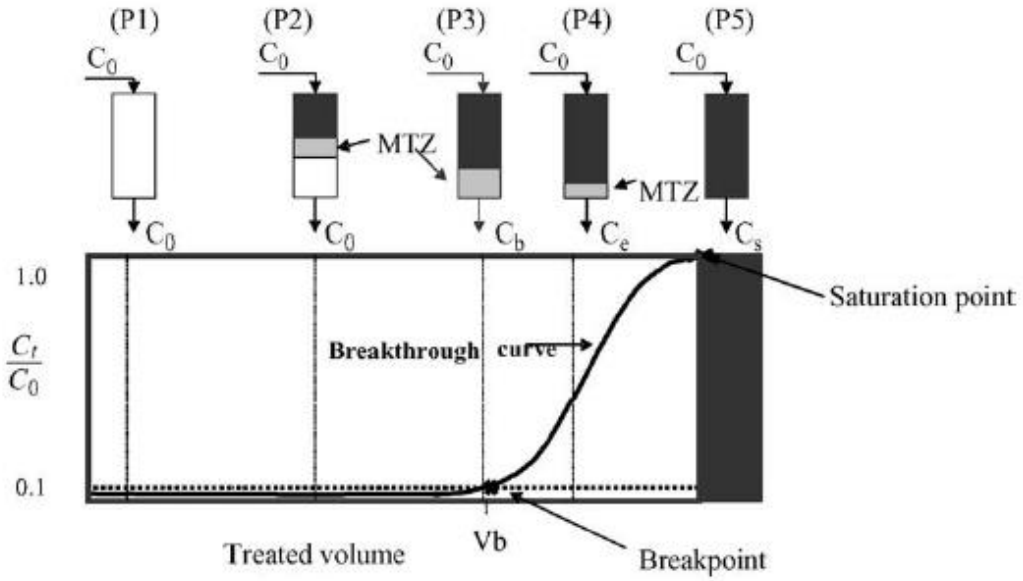

Figure 4.4. Typical breakthrough curve for activated carbon showing the movement of the mass transfer zone according to the throughput volume [100] (MTZ= mass transfer zone).

4.3.3. Materials

4.3.3.1. Adsorbate

All the compounds used to prepare reagent solutions were of analytic reagent grade. The mother solution of lead (1000 mg l^{-1}) was prepared by dissolving a weighed quantity of nitrate lead salt in twice distilled water.

This mother solution was then diluted and the concentrations of metal ions solutions ranged from 1 to 10mg l^{-1}.

Before the solution letting through the column packed with the sawdust, the pH of the solution was adjusted to the required value for the adsorption of lead (II) ions (which was 5.5 according to previous batch study [6]), by adding sodium hydroxide 0.1N or nitric acid 0.1N.

Ionic strength was kept constant at 0.01M value by adding a sodium chloride solution.

The adsorbing potential of sawdust was checked on real effluents supplied by the STCM Company from its industrial site based in Bazoches-les-Gallerandes (45 France).

Beside the metal ion (lead at 1.07 mg l^{-1}) chosen as a model other metal ions (cadmium at 1.73 mg l^{-1}; nickel at 0.30 mg l^{-1} and zinc at 4.70 mg l^{-1}) were found.

4.3.3.2. Adsorbent

The sawdust of *P. sylvestris* used as an adsorbent was provided by the Soci´et´e d'Exploitation Forestiere Barillet, Chˆateauneuf-sur-Loire (45 France).

4.3.3.3. Analysis of lead (II) ions

A Hitachi Z8270 (Perkin Elmer, France) Atomic Absorption Spectrophotometer (AAS) equipped with a Zeeman atomizer and an SSC-300 autosampler was used to determine the concentration of unadsorbed lead (II) ions in the effluent.
Zeeman effect correction and pyrolytic graphite-coated tubes were used for AAS measurements.
All the instrumental conditions were optimized for maximum sensitivity as indicated in a previous study [100].

4.4. Preliminary test on a mini-column

With the purpose of studying the efficiency of packedbed columns in the treatment of a liquid effluent containing lead (II) or other metallic ions, preliminary experiments were carried out on a laboratory scale with a mini-column of 15mminternal diameter (i.d.).
The design of the process is shown in Fig. 4.5.
The aim of this stepwas to improve the process conditions, to minimize the outlet metal ions concentration of the treated effluent, and thus to obtain lower metal ions concentrations than those set by law before dumping.
That is why, the effects of some parameters influencing the adsorption process (bed depth, linear flow rate through the bed and inlet solute concentration) were studied separately.
The results from these experiments were then transposed on a pilot plant scale.
packed beds, respectively, 65, 85 and 130mm in depth.

The column was loaded with dried sawdust, then a 5mm thick layer of glass cotton was placed at the bottom of the column to prevent any loss of biomaterial.

Another one was set at the top of the bed to prevent sawdust dispersion while the solution flowed through the column.

The sawdust particle size used in the fixed-bed studywas inferior to 0.5 mm.

The pH of the feed tank solution was adjusted to 5–5.5 value before feeding the column.

The experiments were carried out at constant room temperature (about 25 ◦C). The columnwas packed vertically while being subjected to vertically directed vibrations to facilitate particle settling and prevent size segregation near the tube walls.

The bottom of the column was connected to a detection cell (DC) equipped with a conductimetric probe (CP), a pH-meter probe (PMP) and a temperature probe (TP). The equilibrium concentration evolution of the solute was monitored by comparing the initial and measured pH values as well as the specific conductivity in the release tanks.

Before letting the solution flow through the bed depth, the column was conditioned with a 0.1M $NaHSO_3$ solution at a pH value of 5.1 contained in the tank (PS), the peristaltic pump (PP2) delivered the latter solution through the bed for 2 h, at a volumetric flow rate of 5ml min^{-1}.

This 2-h pretreatment was necessary to fix the water-soluble compounds of the sawdust and to prevent its extractible polyphenolic compounds from staining the treated water.

The column was then washed for 24 h with distilled water (DW) to clean excess of pre-treatment solution. The column experiments were carried out by feeding a solute solution in down flow mode through the fixed-bed with a peristaltic pump (PP1). Samples collected periodically from the effluent were analyzed by AAS to obtain concentration.

4.5. Pilot plant layout

To compare the bed performance of this process with those of other packed-bed processes, we considered a continuous system able to treat in 4 h a volume of 100 l of solution containing 1mg of lead per liter of polluted solution.

Fig. 4.6 shows the pilot plant column used for these studies. The PVC column (10 cm i.d., 100 cm height with a section of 78.5 cm^2) was used in vertical position. Experiments were carried out with a bed depth of 56 cm. The conditions of application for the experiment were the following ones:

(i) the column was filled up in the same way as the mini-column,

(ii) the column was fed from top to bottom by a centrifugal pump (Kripsol,KS 75 type delivered by Kripsol, Toledo, Spain) equipped with a filter.

This pump delivered 25 l h^{-1} equivalent to a linear flow rate of 5.66 cm min^{-1}. The height of the bed, being of 56 cm, a contact time of about 10 min was estimated to be necessary considering the height of that columns and the lower flow rate.

All the experiments were carried out at room temperature (20–25 ^{0}C).

The breakthrough concentration was defined as the concentration acceptable in view of the limits (10μg l^{-1}) set by the authorities applying to industrial waste before dumping.

Samples of 5ml were regularly taken to monitor the evolution of the metal ions concentration in the outlet solution. They were directly analyzed by AAS without preliminary dilution.

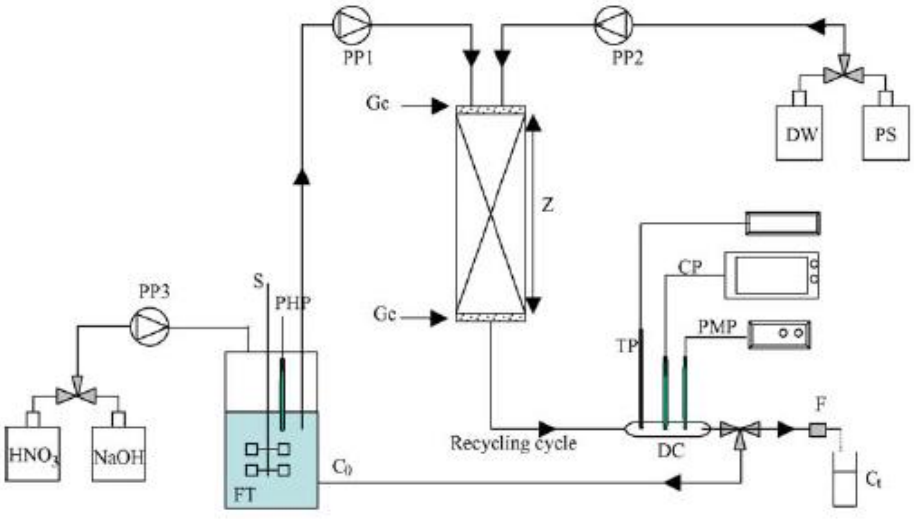

C_0: Initial solute concentration
CP: Conductimetric probe
C_t: Outlet solute concentration at time t
DC: Detection cell
DW: Distilled water
F: Filter
FT: Feed tank
Gc: Glass cotton
PMP: pH-metric probe
PP: Peristaltic pump
PS: Pre-treatment solution
S: Stirrer
TP: Temperature probe
Z: Bed depth

Figure 4.5. Schematic design of column unit for laboratory scale experiments[100]

4.6. Results and discussion

4.6.1. Mini-column scale

The results of lead (II) adsorption onto *P. sylvestris* sawdust are presented in the form of breakthrough curves where the concentration ratio C_t/C_0 is plotted versus time. Several parameters were studied.

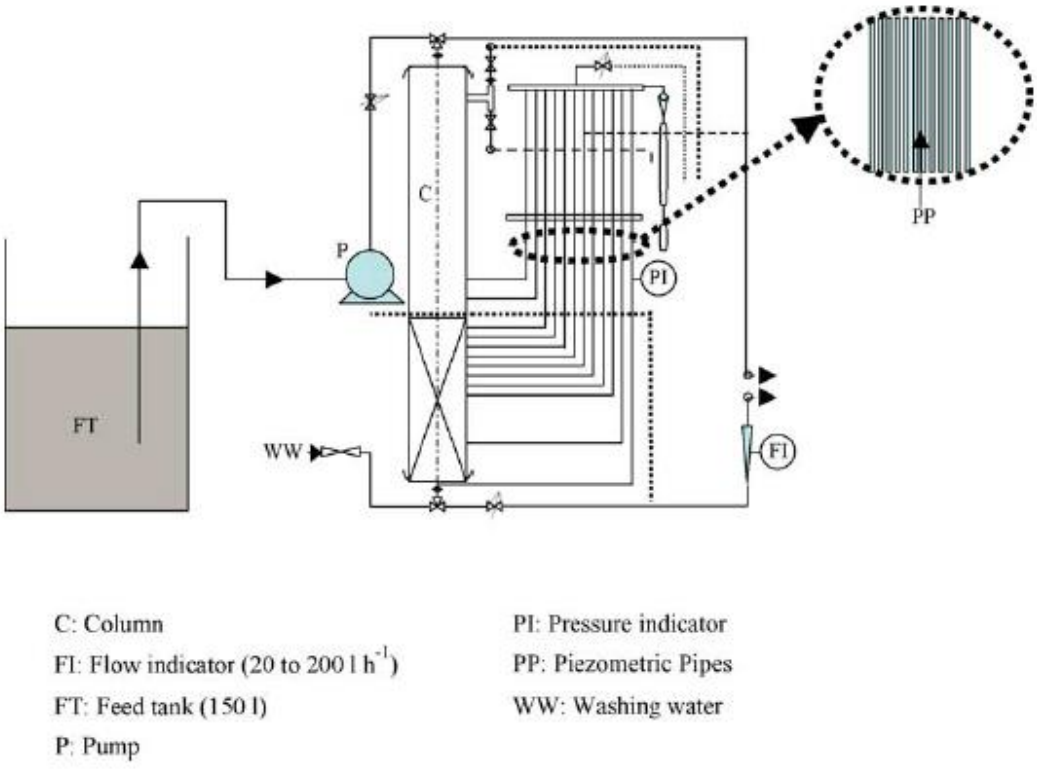

Figure 4.6. Pilot plant setup for industrial wastewater treatment[100]

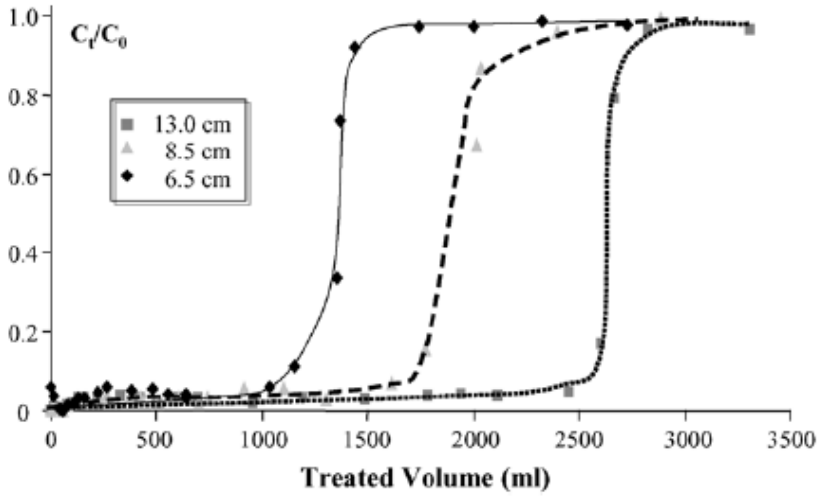

Figure 4.7. Effect of bed depth on the breakthrough curves of lead (II) ions (u = 1.42 cm min^{-1}; C_0 =10mg l^{-1}).[100]

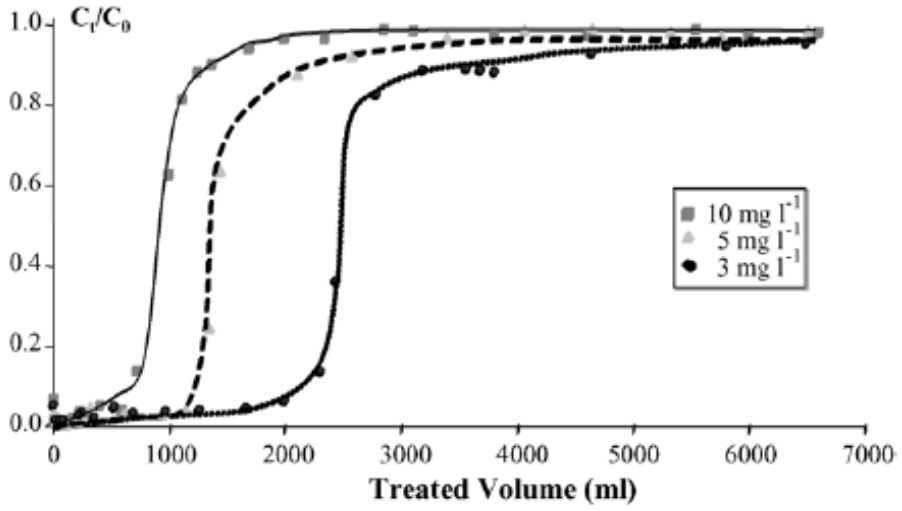

Figure 4.8. Effect of initial concentration onto the breakthrough curves of lead (II) ions (Q_v =10mlmin^{-1}; Z=13 cm; u = 5.66 cm min^{-1})[100]

4.6.1.1. Effect of bed depth

The breakthrough curves obtained for lead (II) ions adsorption are illustrated in Fig. 4.7 above for different bed depth of *P. sylvestris* sawdust (6.5, 8.5, and 13.0 cm), at a constant linear flow rate of 1.42 cm min^{-1}.

They follow the characteristic "S" shape profile produced in ideal adsorption systems.

Results indicate that the breakthrough volume varies with bed depth.

This displacement of the front of adsorption with the increase in depth can be explained by mass transfer phenomena that take place in this process.

When the bed depth is reduced, axial dispersion phenomena predominate in the mass transfer and reduce the diffusion of metallic ions.

The solute (metallic ions) has not enough time to diffuse into the whole of the adsorbent mass. Consequently an important reduction 2580–1110 ml in the volume of solution treated at the breakthrough point is observed when the bed depth in the column decreases from 13.0 to 6.5 cm (Fig. 4.7 and Table 4.2).

Moreover, an increase in the bed adsorption capacity (*q*b) is noticed at the breakthrough point with the increase in bed depth (Table 4.2).

This increase in the adsorption capacity with that in the bed depth can be due to the increase in the specific surface of the adsorbent which supplies more fixation binding sites.

Then it follows that a delayed breakthrough of the pollutant leads to an increase in the volume of solution treated.

The increase in adsorption with that in bed depth was due to the increase in adsorbent doses in larger beds which provide greater service area (or adsorption sites).

Studies of experi-mental conditions (i.e. linear flow rate, bed depth and inlet solute concentration) on the fixation of the metal ions show that the breakthrough time (tb) depends on Z, 1/u and $1/C_0$ according to Eq. (4.8).

The breakthrough time also increased with the height of the bed. Breakthrough time is therefore the determining parameter of the process. The larger it is, the better the intra-particulate phenomena and the bed adsorption capacity are (Table 4.2).

4.6.1.2. Effect of inlet concentration

The effect of a variation from 3 to 10mg l^{-1} of the inlet concentration of the solution used with a linear flow rate of 5.66 cm min^{-1} is shown in Fig. 4.8.

Other results obtained with volumetric flow rates of 1.42 and 2.83 cm min^{-1} showed that the trends of the breakthrough curves were similar.

However, the breakthrough points were totally different.

The effect of the initial concentration onto the breakthrough curves with column bed depth set at 13 cm is shown in Fig. 4.8. It can be seen that a rise in the inlet metal concentration reduces the volume treated before the packed bed gets
saturated as shown in Table 4.2.

A high metal concentration may saturate the sawdust more quickly, thereby decreasing the breakthrough time. Similar results were also obtained for the sorption of copper and cadmium ions onto bone char [13] and sorption of copper and zinc by the residual biomass of the alga *Sargassum* sp. [14].

These results demonstrate that an increase in the concentration modifies the adsorption rate through the bed and increases the bed adsorption capacity (Table 4.2). Therefore the diffusion process depends on the inlet concentration [13,15]. Nevertheless, the saturation of the adsorbent requires much more time.

However the breakthrough is reached before all the active sites of the sawdust are occupied by the metallic ions.

Although, the value of qb obtained in this study was slightly inferior to those obtained in batch system (at a pH value of 5, it was found that qe were 7.14 and 6.29 mg g^{-1} for Pb(II) and Cd(II), respectively).

However, *P. sylvestris* showed in this study a high affinity for lead cations under these experimental conditions.

Table 4.2. Adsorption capacity of sawdust at different initial metal concentrations (Z=13 cm, m_c = 3.92 g u = 5.66 cm. min^{-1}, Qv =10mlmin−1; S_c = 1.77 cm^2)[100]

Initial concentration C_0 (mg l^{-1})	Treated volume V_b (ml)[a]	Breakthrough point t_b (min)[a]	Adsorption bed capacity q_b (mg g^{-1})[b]
3	2200	220	1.7
5	1210	121	1.6
10	850	85	2.2

[a] = Obtained experimentally from Fig. 4.8

[b] = Calculated according to Eq. (4.14).

Table 4. 3. Effect of the linear flow rate on the sorption of lead (II) ions (C_0 =10mg l^{-1}; Z=13 cm; m_c = 3.92 g Sc = 1.77 cm^2) [100]

Linear flow rate u (cm min^{-1})	Treated volume V_b (ml)[a]	Breakthrough time t_b (min)[a]	Adsorption bed capacity q_b (mg g^{-1})[b]
1.42	2580	1030	6.6
2.83	1450	289	3.7
5.66	640	64	1.6

[a] = Obtained experimentally from Fig. 4.9

[b] = Calculated according to Eq. (4.14)

4.6.1.3. Effect of the linear flow rate

The fact that the section area of the column is uniform implies that the linear flow rate through the bed, u, is directly proportional to the overall volumetric flow rate through the packed bed (u =Qv/Sc) [101].

To examine the effect of the linear flow rate through the bed depth, the initial solute concentration and bed depth were kept constant (C_0 =10mg l^{-1}, Z = 13 cm) while the linear flow rate varied from 1.42 to 5.66 cm min^{-1}.

Results are given in Fig. 4.9 and show that the uptake of metal ions onto the biomaterials decreases when the linear flow rate through the bed increases.

An increase in the linear flow rate reduces the volume treated efficiently until breakthrough point and therefore decreases the service time of the bed.

This is due to the decrease in contact time between the metal ions and the sawdust at higher linear flow rates.

As the adsorption rate is controlled by intra-particulate diffusion, an early breakthrough occurs leading to a low bed adsorption capacity (Table 4.3).

These results are also in agreement with those referred to the literatures [101].

When the linear flow rate decreases the contact time in the column is longer, intra particulate diffusion then becomes effective.

Thus the metallic ions have more time to diffuse amidst the particles of sawdust and a better adsorption capacity is obtained (Table 4.3).

At a higher linear flow rate, the biosorbent gets saturated early, certainly because of a reduced contact time, a larger amount of ions adsorbed on the sawdust and a weak distribution of the liquid into the column, which leads to a lower diffusivity of the solute amidst the particles of the biomaterials.

This shows an increase in the uptake of the metallic ions due to the intra-particulate phenomena.

Therefore the volume treated, the breakthrough time and the bed adsorption capacity were reduced and a wide volume of solution is purified with an efficient elimination. As can be seen in Table4.3, 2580 ml of solution were treated at a low linear flow rate of 1.42 cm min^{-1} while 640 ml were treated at a high linear flow rate of 5.66 cm min^{-1}.

Similar effect by studying the elimination of copper using the calcium alginates and gold using microorganisms were also presented [101].

4.6.1.4. Application of the BDST model with variations in the initial solute concentration

The effect of the inlet initial concentration on bed performance was studied through the BDST model.

The results obtained are presented in Fig.4.10 by a plot of service time versus bed depth at a constant linear flow rate.

They show that an increase in slope when the inlet metal ions concentration decreases, allowing to treat a larger volume of solution. The variation of inlet concentration also affects the BDST parameters.

The adsorption capacity values, calculated according to Eq. (4.8), slightly increase with inlet concentration (Table 4.4) and the dynamic bed capacity of the column (N_0) increases by about 36% when the inlet concentration varies from 3 to 10 mg l^{-1}.

These results are in correlation with those observed when studying the breakthrough curves and explain the lower performance obtained when concentration is raised.

Correlation coefficients calculated by the linearization of experimental data are superior to 0.92 (Table 4.4).

Table 4.5 gives the results obtained from slopes and intercepts at constant linear flow rate and particle size, by calculations from eqs. (4.9) and (4.10).

These results were compared with those obtained experimentally.

The predicted BDST parameters calculated from the slope and intercept of the median for the highest and lowest inlet concentrations, using Eq. (4.9), show a good agreement with those obtained experimentally with a correlation coefficient superior to 0.98.

The experimental error was around 11%. Therefore, from these results we could conclude that the BDST model can produce accurate prediction for the variations of inlet concentration in a dynamic process for lead or other metallic ions–sawdust systems.

This model was also successfully used for the prediction of the breakthrough curves in the elimination of lead and cadmium and were in agreement with the previous studies [101].

The results obtained in the above described experiments were very encouraging and suggested *P. sylvestris* sawdust offers real potentialities as an ionic-exchanger for an application of the process in industrial plants for the treatment of real

liquid effluents as reported previously [101].

An application of the process on a pilot plant was then considered to validate the process and to find the optimal conditions.

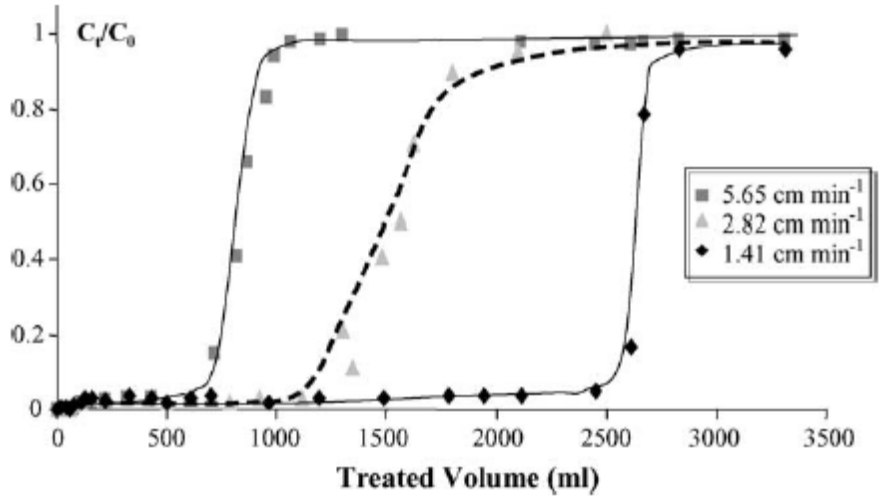

Figure 4.9. Effect of the linear flow rate onto the breakthrough curves of lead (II) ions (Z=13 cm; C_0 =10mg l^{-1}). [101]

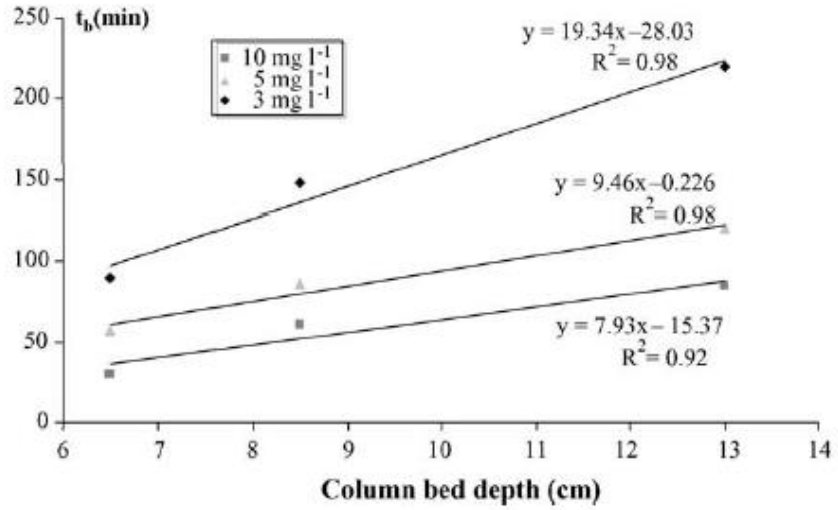

Fig. 4.10. Effect of inlet concentration onto the sorption of lead (II) ions: BDST modelling (u = 5.66 cm min^{-1}).[101]

Table 4.4. Effect of inlet concentration on the BDST parameters (u = 5.65 cm min^{-1}; Sc = 1.77 cm^2; m_c = 3.92 g) [101]

Inlet concentration C_0 (mg l^{-1})	Adsorption capacity q_b (mg g^{-1})[a]	Constant k_{ads} (l mg^{-1} min^{-1})[b]	Dynamic capacity N_0 (mg l^{-1})[c]	R^2
3	1.7	0.026	328	0.98
5	1.6	1.944	268	0.98
10	2.2	0.014	449	0.92

For all experiments the ratio C_0/C_b was 10. R^2 is the Correlation coefficient.

[a] Calculated according to Eq. (4.14) (Table 4.2).

[b] Obtained according to the abscissa intercept in BDST plot (Fig. 4.10 and Eq. (4.8)).

[c] Obtained according to the slope in BDST plot (Fig. 4.10 and Eq. (4.8)).

Table 4.5. Constants of BDST model calculated and obtained experimentally (u = 5.65 cm min^{-1}; Sc = 1.77 cm^2) [101]

Inlet concentration C_0 (mg l^{-1})	Analyze	Slope m_x (min cm^{-1})	Intercept, C_x (min)	Dynamic capacity N_0 (mg l^{-1})	R^2
3	Experimental	19.34[a]	−28.03[a]	328	0.99
5	Experimental	9.46[a]	−0.23[a]	268	0.98
10	Experimental	7.93[a]	−15.37[a]	449	0.92
10	Calculated	7.02[b]	−13.20[b]	399	1.00

R^2 is the correlation coefficient.

[a] Obtained experimentally from Fig. 4.10.

[b] Obtained according to Eqs. (4.11) and (4.12), respectively, for m_x and C_x.

4.6.2. Pilot plant scale

For the model building of systems using biomaterials as adsorbents in continuous systems, residence time is an important parameter.

The longer the residence time is, the better the bed performance is. In our system we can reach the highest residence time in two ways:

(i) by increasing the height of the column, which allows increasing the contact time;

(ii) by decreasing the linear flow rate through the column, which increases the contact time.

The linear flowrate through the bed depth was chosen according to the mini-column results.

For scale-up experiments we increased the internal diameter (*D*i) as well as the bed depth (*H*) while keeping constant the ratio *D*i/*H*at a value of 0.18.

This value corresponds to the 85mm high mini-column of 15mm in internal diameter and the linear flow rate through the column was maintained constant at 5.3 cm min^{-1} (corresponding to a volumetric flow rate of 25 l h^{-1}).

Comparison of geometric and operating parameters used with mini and pilot columns are indexed in Table 4.6.

BDST parameters, k_{ads} (adsorption rate constant) and N_0 (dynamic adsorption capacity), calculated from mini-column experiments were used to predict the service time of the column for the scale-up experiment.

The experimental results about the breakthrough curves of the adsorption of lead (II) obtained by measuring the outlet lead (II) ions concentrations are shown in Fig. 4.11which presents the Ct/C_0 $f(t)$ function.

Initially, the concentration of metal ions adsorbed by the bed and that of the solution leaving the column are equal to 0.

However, after a contact time of 45 h, which corresponds to 10% of the breakthrough point, the metal begins to flow through the column outlet.

This time agrees with the service time of the sawdust. Then the concentration increases gradually until $Ct = C_0$, and at this moment the bed is saturated.

The service time of the column defined at 10% of breakthrough point is given in Table 4.7.

Results show that the service times (t_b) deduced from the BDST model and those obtained experimentally are of the same order.

In spite of the presence of other metal ions in the industrial effluent, the breakthrough curves (Fig. 4.11) evolve in the same way.

This experiment was not carried on until saturation was reached because the firm could not supply any more effluent.

According to the results obtained, it was noticed that the BDST model applied to 10% of breakthrough point allows to simulate or to predict the experimental breakthrough time with a relatively weak abnormality with regard to the theoretical value.

Table 4.6 . Data of parameters used for laboratory and pilot experiments[101]

Parameters	Mini-column	Pilot column	Scale-up ratio
Geometric			
Internal diameter (cm)	1.5	10	6.7
Section (cm^2)	1.77	78.5	44.4
Height (cm)	15	100	6.7
Operating			
Linear flow rate ($cm\,min^{-1}$)	5.6	5.3	0.95
Inlet concentration ($mg\,l^{-1}$)	10	10	1
Volumetric flow ($l\,h^{-1}$)	0.6	25	41.7
Height of sawdust bed (cm)	8.5	56	6.6
Adsorbent weight (g)	3.9	1000	256

Table 4.7. Comparison of the dynamic data predicted from the BDST model with those obtained experimentally [101]

Effluent	Treated volume (l)	Calculated service time t_b (h)	Predicted service time (h)		Deviation (%)	Uptake (%
			$C_0 = 3\,mg\,l^{-1}$	$C_0 = 10\,mg\,l^{-1}$		
Industrial	NS	NS	45	45	NS	99.9[a]
Synthetic	1150	46	48	48	4	99.9[a]

NS: not specified.

[a] Corresponds approximately to 1.25–2 g of lead (II) per kg of sawdust starting from the initial concentration of 1.07 mg l^{-1}.

CONCLUSIONS

Fixed-bed or column adsorption is the most popular option in practical application of adsorption process, and due to the complexity of a column adsorption system and lack of solid theory, its mathematical modeling is obviously more difficult than batch adsorption.

To choose or develop a suitable model, accuracy and convenience should be considered simultaneously.

Currently, although some effort had been made to complete these models (especially the general rate models and LDF model), each model has its inherent shortages and requires further development.

The general rate models (and "general rate type" models) and LDF model generally fit well with the experimental data for most cases, but they are relatively time-consuming.

Other models including the Bohart-Adams model, Yoon-Nelson model, Thomas model, Wang model, Wolborska model, and modified dose-response model could be applicable without isotherm information, but they are derived from specific situations and limited in space.

The Clark model is suitable to describe column adsorption obeying the Freundlich isotherm and do not show conspicuously better accuracy than the above models.

The constant pattern model is relatively convenient to apply and gives satisfactory prediction, but it cannot be readily employed for adsorption predominated by intrapellet diffusion.

In addition, experimental work is always required to determine the isotherm and dynamic model as well as the related parameters.

Moreover, when the breakthrough curve deviates from the ideal S shape, prediction derived from any model usually cannot meet our demand.

In case study 1, i.e. copper biosorption on immobilized seaweed biomass, that is the biosorption of copper by the brown seaweed *Sargassum baccularia*, immobilized onto polyvinyl alcohol (PVA) gel beads, it has demonstrated that seaweed biomass immobilized in PVA gel was compatible with fixed-bed column operation for copper removal.

A positive aspect of this biosorbent was that it exhibited favorable regeneration conditions, with nearly complete regeneration achieved with aqueous solution containing EDTA.

The metal uptake property of the biosorbent remained practically unaltered during three successive cycles of biosorption-desorption.

The Bohart-Adams model was used to describe breakthrough profiles obtained at di erent flow rates and feed concentrations.

Calculated breakthrough curves of the model were in approximate agreement with the experimental ones. It was established that the column behavior of this biosorbent was not entirely predictable on the basis of the simplistic Bohart-Adams model. A more detailed analysis using mass transfer models will be the subject of future communications.

In case study 2, that is the adsorption of lead (II) ions through sawdust in a packed bed column, and, especially, the removal of lead (II) ions from effluents using immobilized *Pinus sylvestris* sawdust, is an economically feasible technique for removing metal ions from a solution.

The process allows treatment of a given volume of effluent by using a minimal mass of adsorbent which concentrates maximal content of metal.

The adsorption breakthrough curves obtained at different flow rates indicate that an increase in flow rate decreases the volume treated until the breakthrough point and therefore decreases the service time of the bed.

Lower removal capacities were observed, probably due to the fact that contact times were insufficient for the adsorption equilibrium to develop between the sawdust and the metal ions.

This process was applied to industrial effluents containing some lead in the presence of other metallic ions (nickel, copper, cadmium, zinc, iron).

The application of the BDST model at 10% of breakthrough point gave satisfactory results with an error of around 4% with regard to the theoretical service time.

This model was used to scale-up the process from a 0.6 l h^{-1} output (u = 5.6 cm min^{-1}) with the mini-column to a 25lh^{-1} one (u = 5.3 cm min^{-1}) with the pilot column (Table4.6).

Moreover we were able to increase the flow rate to 100 l of solution per hour, which indicated that sawdust adsorption could successfully reduce the metallic ion concentration of outlet industrial effluents in packed bed columns.

The results obtained with the pilot show that the process can decontaminate 1200 l of effluent containing 1mg l−1 of lead (II) with only 1 kg of sawdust, before the pollutant gets released.

Thus, the process can adsorbe approximately 1.25–2 g of diluted lead (II) per kilogram of sawdust, with a 99% removing efficiency.

Moreover, the pollutant adsorbed on the cheap material can be then captured since the polluted sawdust can be burnt in industrial furnaces and lead can be recovered from the ashes after a chemical treatment.

Inexpensive, effective, readily available materials can be used in place of activated carbon or ion-exchange resins for the removal of heavy metals from solution. Therefore, comparisons of the adsorbents are difficult because of inconsistencies in data presentation.

However, from the literature reviewed, the sorbent used in this study was compared in term of cost with those that stand out for high absorbency such as activated carbon, fungi biomass, ion-exchange resins, marine algae.

Although, improved sorption capacity may compensate the cost of additional processing it was noticed that the sawdust presented a better option with a complete reusability, lower purchase price, biodegradable, by-product and easy handling.

BIBLIOGRAPHY

1. Seader, J.D. and Henley, Ernest J. (2006). Separation Process Principles (2nd Edition ed.). John Wiley & Sonstahm. ISBN 0-471-46480-5.
2. Fogler, H. Scott (2006). Elements of Chemical Reaction Engineering (4th Edition ed.). Prentice Hall. ISBN 0-13-047394-4.
3. Perry, Robert H. and Green, Don W. (1984). Perry's Chemical Engineers' Handbook (6th Edition ed.). McGraw-Hill. ISBN 0-07-049479-7.
4. Ergun, Sabri. "Fluid flow through packed columns." Chem. Eng. Prog. 48 (1952).
5. J. Kozeny, "Ueber kapillare Leitung des Wassers im Boden." Sitzungsber Akad. Wiss., Wien, 136(2a): 271-306, 1927.
6. P.C. Carman, "Fluid flow through granular beds." Transactions, Institution of Chemical Engineers, London, 15: 150-166, 1937.
7. Barros, M.A.S.D., Zola, A.S, Tavares, C.R.G., Sousa-Aguiar, E.F. Chromium uptake from tricomponent solution in zeolite fixed bed, Adsorption, 12, 229-248, 2006.
8. Barros, M.A.S.D., Silva, E.A., Arroyo, P.A., Tavares, C.R.G., Schneider, R.M., Suszek, M., Sousa-Aguiar, E.F., Removal of Cr(III) in the fixed bed column and batch reactors using as adsorbent zeolite NaX, Chemical Engineering Science, 59, 5959 – 5966, 2004.
9. McCabe, W. L., Smith, J.C., and Harriot, P.”Unit Operations of Chemical Engineering”,McGraw-Hill International Ed., 6th ed., New York, USA, 2001.
10. Helferich, F.,Ion Exchange, Dover Publications Inc., New York, 1995.
11. Sánchez, A., Ballester, A., Blásquez, M.L., González, F., Muñoz, J., Hammaini, A.: Biosorption of copper and zinc by cymodocea nodosa. FEMS Microbiol. Rev. 23 527-536 (1999).
12. Myers, A. L.; Prausnitz, J. M.; Thermodynamics of mixed-gas adsorption; AIche Journal, 11, 1, 121-127, 1965.
13. Geankoplis, C.J., Transport Processes andUnit Operations, 3rd ed., PTR Prentice Hall, USA, 1993.
14. Walker, G.M., Weatherly, L.R. Adsorption of acid dyes on to granular activated carbon in fixed beds, Water Research, 31, 8, 2093–2101, 1997.

15. Gazola, F. C., Pereira, M.R., Barros, M.A.S.D, Silva, E.A, Arroyo, P.A. Removal ofCr3+ in fixed bed using zeolite NaY, Chemical Engineering Journal, 117, 253–261,2006.
16. Fogler, H.S., Elements of Chemical Reaction Engineering, 3rd ed., Prentice Hall, New Delhi- India, 2004.
17. Hill, C.G.,"An Introduction to Chemical Engineering Kinetics and Reactor Design,' John Wiley & Sons, USA, 1977.
18. Barros, M,A,S,D, Zola, A,S., Arroyo, P.A., Sousa-Aguiar, E.F., Tavares, C.R.G. Binary Ion Exchange of Metal Ions in Y and X Zeolites, Brazilian Journal of Chemical Engineering, 20, 4, 413-421, 2003.
19. Valdman, E., Erijman, L., Pessoa, F.L.P. and Leite, S.G.F. Continuous Biosorption of Cu and Zn by Immobilized Waste Biomass Sargassum sp., Process Biochemistry, 36, 869-873, 2001.
20. Mohan, D. and Chander, S., Single Component and Multi-component Adsorption of Metal Ions by Activated Carbons, Colloids and Surfaces A: Physicochemical and Engineering Aspects, 177, 2-3, 183-196, 2001.
21. KLamer, K, Van Krevelen, D. W., Studies on ion Exchange-I, Chem. Eng. Sci, 7, 4, 197-203, 1958.
22. Barros, M.A.S.D., Zola, A.S., Arroyo, P.A., Sousa-Aguiar, E.F., Tavares, C.R.G.Equilibrium and dynamic ion exchange studies of Cr3+ on zeolites NaA and NaX, Acta Scientiarum, 24, 6, 1619-1625, 2009.
23. Bohart, G. S., Adams, E. Q., Some aspects of the behavior of charcoal with respect to chlorine,Journal of the American Chemical Society, 42, 523-544, 1920.
24. Thomas, H.C., Heterogeneous ion exchange in a flowing system, Journal of the American Chemical Society, 66, 1664–1666, 1944.
25. Hsuen, H. K., An improved linear driving force approximation for intraparticle adsorption, Chemical Engineering Science, 55,3475-3480, 2000.
26. Delgado, J.M.P.Q., A critical review of dispersion in packed bed, Heat Mass Transfer, 42, 279-310, 2006.
27. Ostroski, I.C., Mechanism of removal of Iron(III) and Zinc(II) ontoZeolite Na-Y, In Portuguese, Master Thesis, UEM - State University of Maringá, Brazil,Chemical Engineering Department , 2007.

28. Abu-Lail, L., Bergendahl, J.A., Thompson, R.W., 2012.Mathematical modeling of chloroform adsorption ontofixed-bed columns of highly siliceous granular zeolites.*Environmental Progress & Sustainable Energy*, **31**(4):591-596. [doi:10.1002/ep.10593]
29. Zhao, Y., Shen, Y.M., Bai, L., Ni, S.Q., 2012. Carbon dioxideadsorption on polyacrylamide-impregnated silica gel andbreakthrough modeling. *Applied Surface Science*, **261**:708-716. [doi:10.1016/j.apsusc.2012.08.085]
30. Cheknane, B., Baudu, M., Bouras, O., Zermane, F., 2012. Modeling of basic green 4 dynamic sorption onto granularorgano-inorgano pillared clays (GOICs) in column reactor.*Chemical Engineering Journal*, **209**:7-12. [doi:10.1016/j.cej.2012.07.118]
31. Crittenden, J.C., Hutzler, N.J., Geyer, D.G., Oravitz, J.L.,Friedman, G., 1986. Model development and parametersensitivity. *Water Resources Research*, **22**(3):271-284.[doi:10.1029/WR022i003p00271]
32. Helfferich, F.G., 1995. Ion Exchange, Dover Pubns.
33. Fournel, L., Mocho, P., Brown, R., le Cloirec, P., 2010. Modeling breakthrough curves of volatile organic compounds on activated carbon fibers. *Adsorption*, **16**(3):147-153.
34. Warchoł, J., Petrus, R., 2006. Modeling of heavy metal removal dynamics in clinoptilolite packed beds. *Microporous and Mesoporous Materials*, **93**(1-3):29-39. [doi:10.1016/j.micromeso.2006.01.021]
35. Malek, A., Farooq, S., 1996. Comparison of isotherm models for hydrocarbon adsorption on activated carbon. *AIChE Journal*, **42**(11):3191-3201. [doi:10.1002/aic.690421120]
36. Medved, I., Cerny, R., 2011. Surface diffusion in porous media:A critical review. *Microporous and Mesoporous Materials*, **142**(2-3):405-422.
37. Langmuir, I., 1916. The constitution and fundmental properties of solids and liquids. part I. Solids. *Journal of the American Chemical Society*, **38**(11):2221-2295. [doi:10.1021/ja02268a002]
38. Giles, C., MacEwan, T., Nakhwa, S.N., 1960. Studies inadsorption. Part XI. A system of classification of solutionadsorption isotherms, and its use in diagnosis ofadsorption mechanisms and in measurement of specificsurface areas of solids. *Journal of the Chemical Society*,(0):3973-3993. [doi:10.1039/jr9600003973]

39. Azizian, S., 2004. Kinetic models of sorption: a theoretical analysis. *Journal of Colloid and Interface Science*, **276**(1):47-5[doi:10.1016/j.jcis.2004.03.048]
40. Haghseresht, F., Lu, G., 1998. Adsorption characteristics of phenolic compounds onto coal-reject-derived adsorbents.*Energy & Fuels*, **12**(6):1100-1107. [doi:10.1021/ef9801165]
41. Du, X., Yuan, Q., Li, Y., 2008. Mathematical analysis ofsolanesol adsorption on macroporous resins using thegeneral rate model. *Chemical Engineering & Technology*,**31**(9):1310-1318. [doi:10.1002/ceat.200800010]
42. Tien, C., 1994. Adsorption Calculations and Modeling.Butterworth-Heinemann Boston.
43. Liu, B., Zeng, L., Ren, Q., 2010. Simulation of levulinic acidadsorption in packed beds using parallel pore/surfacediffusion model. *Chemical Engineering & Technology*,**33**(7):1146-1152. [doi:10.1002/ceat.201000147]
44. Plazinski, W., Rudzinski, W., Plazinska, A., 2009. Theoreticalmodels of sorption kinetics including a surface reactionmechanism: a review. *Advances in Colloid and Interface Science*, **152**(1-2):2-1[doi:10.1016/j.cis.2009.07.009]
45. Glueckauf, E., 1955. Theory of chromatography. Part 10.—Formulæ for diffusion into spheres and their applicationto chromatography. *Transactions of the Faraday Society*,**51**(0):1540-1551. [doi:10.1039/tf9555101540]
46. Worch, E., 2008. Fixed-bed adsorption in drinking watertreatment: a critical review on models and parameter estimation.*Journal of Water Supply Research and Technology—AQUA*, **57**(3):171-183. [doi:10.2166/aqua.2008.100]
47. Szukiewicz, M.K., 2002. An approximate model for diffusionand reaction in a porous pellet. *Chemical EngineeringScience*, **57**(8):1451-1457. [doi:10.1016/S0009-2509(02)00055-6]
48. Gholami, M., Talaie, M., 2010. Investigation of simplifyingassumptions in mathematical modeling of natural gasdehydration using adsorption process and introduction ofa new accurate LDF model. *Industrial & EngineeringChemistry Research*, **49**(2):838-846. [doi:10.1021/ie901183q]
49. Clark, R.M., 1987. Evaluating the cost and performance offield-scale granular activated carbon systems. *EnvironmentalScience & Technology*, **21**(6):573-580. [doi:10.1021/es00160a008]

50. Ghasemi, M., Keshtkar, A.R., Dabbagh, R., Jaber Safdari, S.,2011. Biosorption of uranium (VI) from aqueous solutions by Ca-pretreated Cystoseira indicaalga: breakthrough curves studies and modeling. *Journa of Hazardous Materials*, **189**(1-2):141-149 [doi:10.1016/j.jhazmat.2011.02.011]
51. Aksu, Z., Gönen, F., 2004. Biosorption of phenol byimmobilized activated sludge in a continuous packed bed:prediction of breakthrough curves. *Process Biochemistry*,**39**(5):599-613. [doi:10.1016/S0032-9592(03)00132-8]
52. Ko, D.C.K., Porter, J.F., McKay, G., 2000. Optimised correlations for the fixed-bed adsorption of metal ions on bone char. *Chemical Engineering Science*, **55**(23):5819-5829. [doi:10.1016/S0009-2509(00)00416-4]
53. Bohart, G. S., Adams, E. Q. (1920). Some aspects of thebehaviour of charcoal with respect to chlorine. J. Am. Chem.Soc., **42**, 523-529.
54. Hutchins, R., 1973. New method simplifies design of activated carbon systems. *Chemical Engineering*, **80**(19):133-138.
55. McKay, G., 1979. Basic dye adsorption on activated carbon.*Water, Air, & Soil Pollution*, **12**(3):307-317. [doi:10. 1007/BF01047018]
56. Wilson, E., Geankoplis, C., 1966. Liquid mass transfer at verylow Reynolds numbers in packed beds. *Industrial & Engineering Chemistry Fundamentals*, **5**(1):9-14. [doi:10. 1021/i160017a002]
57. Yoon, Y.H., James, H.N., 1984. Application of gas adsorptionkinetics I. A theoretical model for respirator cartridgeservice life. *The American Industrial Hygiene AssociationJournal*, **45**(8):509-516. [doi:10.1080/15298668491400197]
58. Hamdaoui, O., 2006. Dynamic sorption of methylene blue bycedar sawdust and crushed brick in fixed bed columns.*Journal of Hazardous Materials*, **138**(2):293-303.[doi:10.1016/j.jhazmat.2006.04.061]
59. Wang, Y.H., Lin, S.H., Juang, R.S., 2003. Removal of heavy metal ions from aqueous solutions using various low-costadsorbents. *Journal of Hazardous Materials*, **102**(2-3):291-302. [doi:10.1016/S0304-3894(03)00218-8]
60. Wolborska, A., Pustelnik, P., 1996. A simplified method fordetermination of the break-through time of an adsorbentlayer. *Water Research*, **30**(11):2643-2650. [doi:10.1016/S0043-1354(96)00166-2]

61. Araneda, C., Basualto, C., Sapag, J., Tapia, C., Cotoras, D.,Valenzuela, F., 2011. Uptake of copper (II) ions fromacidic aqueous solutions using a continuous column packed with microcapsules containing a β-hydroxyoximic compound. *Chemical Engineering Research & Design*,**89**(12):2761-2769. [doi:10.1016/j.cherd.2011.05.008]
62. Rao JR, Viraraghavan T. Biosorption of phenol from a aqueoussolution by *Aspergillus niger* biomass. Bioresour Technol 2002;85:165–71.
63. Aksu Z, Akpinar D. Modelling of simultaneous biosorption of phenoland nickel(II) onto dried aerobic activated sludge. Sep Pur Technol 2000;21:87–99.
64. Texier AC, Andres Y, Faur-Brasquet C, LeCloirec P. Fixed-bed studyfor lanthanide (La, Eu, YB) ions removal from aqueous solutionsby immobilized *Pseudomonas aeruginosa*: experimental data and modelization. Process Biochem 2002;47:333–42.
65. Aksu Z, Gönen F, Demircan Z. Biosorption of chromium(VI) ions by Mowital®B30H resin immobilized activated sludge in a packed bed: comparison with granular activated carbon. Process Biochem 2002;38:175–86.
66. N. Akhtar, J. Iqbal, M. Iqbal, Removal and recovery of nickel (II) fromaqueous solution by loofa sponge-immobilized biomass of *Chlorelasorokiniana*: characterization studies, J. Hazard. Mater. B108 (2004) 85–94.
67. B. Volesky, Biosorption of Heavy Metals, CRC Press, Boston/Boca Raton, FL, 1990.
68. E.W. Wilde, J.R. Benemann, Bioremoval of heavy metals by use of microalgae, Biotechnol. Adv. 11 (1993) 781–812.
69. E. Sandau, P. Sandau, O. Pulz, Heavy metal sorption by microalgae, Acta Biotechnol. 16 (1996) 227–235.
70. K.H. Chong, B. Volesky, Description of two-metal biosorption equilibria by Langmuir type models, Biotechnol. Bioeng. 47 (1995) 451–460.
71. S. Schiewer, B. Volesky, Modelling multi-metal ion exchange in biosorption Environ. Sci. Technol. 30 (1996) 2921–2927.
72. M.T. Veit, C.R.G. Tavares, E.A. Silva, Influence of pH and pre-treatedbiomass *Sargassum filipendula* in organic leaching, in: Anais do II Congresso Brasileiro de Termodinˆamica Aplicada, 2004

73. E.A. Silva, E.S. Cossich, C.R.G. Tavares, L. Cardozo, R. Guirardello,Modeling of copper (II) biosorption by marine alga *Sargassum* sp. infixed bed column, Process Biochem. 38 (2002) 791–799.
74. D. Kratochvil, B. Volesky, Advanceds in biosorption of heavy metals, Trends Biotechnol. 16 (1998) 291–300
75. E.A. Silva, C.R.G. Tavares, M.A.S.D. Barros, P.A. Arroyo, R.M. Schneider,M. Suszek, Modeling and experimental Cr+3 uptake using NaXzeolite, in: Sixth Italian Conference on Chemical and Process Engineering 2003, Pisa, Italy, Chem. Eng. Trans. 3 (2003) 303–308.
76. G. McKay, M.J. Bino, Fixed bed adsorption for the removal of pollutants from water, Environ. Pollut. 66 (1990) 33–53.
77. D.C.K. Ko, J.F. Poter, G. Mackay, Optimised correlations for the fixedbed adsorption of metal ions on bone char, Chem. Eng. Sci. 55 (2000) 5819–5829.
78. S.M. Robinson, W.D. Arnold, C.H. Byers, Mass-transfer mechanismsfor zeolite ion exchange in wastewater treatment, Environ. Energy Eng.40 (1994) 2045–2053.
79. G.S. Bohart, E.Q. Adams, Some aspects of the behavior of charcoal with respect to chlorine, J. Am. Chem. Soc. 42 (1920) 523–544.
80. H.C. Thomas, Heterogeneous ion exchange in a flowing system, J. Am. Chem. Soc. 66 (1944) 1664–1666.
81. M. Otero, M. Zabkova, A.E. Rodrigues, Comparative study of adsorption of phenol and salicylic acid from aqueous solution onto nonionic polymeric resins, Sep. Purif. Technol. 45 (2005) 86–95.
82. M.A.S.D. Barros, E.A. Silva, P.A. Arroyo, C.R.G. Tavares, R.M. Schneider, M. Suszek, E.F. Sousa-Aguiar, Removal of Cr(III) in the fixed bed column and batch reactors using as adsorbent zeolite NaX, Chem. Eng. Sci. 59 (2004) 5959–5966.
83. S. Brosillon, M.H. Manero, J.N. Foussard, Mass transfer in VOC adsorption on zeolite: experimental and theoretical breakthrough curves, Environ. Sci. Technol. 35 (2001) 3571–3575
84. E.M. Trujillo, T.H. Jeffers, C. Ferguson, H.Q. Stevenson, Mathematically modeling the removal of heavy metals from a wastewater using immobilized biomass, Environ. Sci. Technol. 25 (1991) 1559–1565.

85. F.X. Stuart, D.T. Camp, Comparison of kinetic and diffusional models for packed bed adsorption, I. C. Fundam. 6 (1967) 156–158.
86. J.S.C. Hsieh, R.M. Turian, C. Tien, Multicomponent liquid phase adsorption in fixed bed, AIChE J. 23 (1977) 263–275.
87. M.V. Ernest Jr., R.D. Whitley, Z. Ma, N.H.L. Wang, Effects of mass action equilibria on fixed bed multicomponent ion exchange dynamics, Ind. Eng. Chem. Res. 36 (1997) 212–226.
88. Mehta S K, Gaur J P, 2005. Use of algae for removing heavymetal ions from wastewater: progress and prospects[J]. Crit Rev Biotechnol, 25: 113–152.
89. Zemke-WhiteWL, Ohno M, 1999.World seaweed utilization: an end-of-century summary[J]. J Appl Phycol, 11: 369–376.
90. Xian X, Qiu H Y, Cai Z Z *et al*., 2006. The research on theadsorption e_ect on metal ions by immobilized marine algae[J]. Acta Oceanologica Sinica, 25: 153–158.
91. Cossich E S, da Silva E A, Tavares C R G *et al*., 2004. Biosorption of chromium(III) by biomass of seaweed *Sargassum* sp. In a fixed-bed column[J]. Adsorption, 10: 129–138.
92. Chen K C, Lin Y F, 1994. Immobilization of microorganisms with phosphorylated polyvinyl alcohol (PVA) gel[J]. Enzyme Microb Technol, 16: 79–83.
93. Cooney D O, 1999. Adsorption design for wastewater treatment[M]. Boca Raton: Lewis Publishers.
94. Ruthven D M, 1984. Principles of adsorption and adsorption processes[M]. New York: Wiley
95. G. Rich, K. Cherry, Cited in Hazardous Waste Treatment Technology, Pudvan Publishing Co., New York, 1987.
96. A.K. Bhattacharya, C. Venkobachar, J. Environ. Eng.—ASCE 110 (1984) 110–122.
97. C. Huang, C.P. Huang, Water Res. 30 (1996) 1985–1990.
98. J.M. Brady, J.M. Tobin, J.C. Roux, J. Chem. Technol. Biotechnol. 74 (1999) 71–77.

99. V.C. Taty Costodes, H. Fauduet, C. Porte, A. Delacroix, Proceedingsof the 12th European Conference and Technology Exhibition on Biomass for Energy Industry and Climate Protection, Amsterdam, The Netherlands, 17–21 June, 2002

100. V.C. Taty Costodes, H. Fauduet, C. Porte, A. Delacroix, J. Hazard.Mater. 105 (2003) 121–142.

101. A.V. Pethkar, K.M. Paknikar, J. Biotechnol. 55 (1998) 121–136.

.